Interaction Notes

Note 441

9 July 1984

Multiple Parallel Wires Above A Finitely Conducting Plane Earth In The Presence Of A Plane Wave (EMP)*

H. P. Neff, Jr.
University of Tennessee
Knoxville, Tennessee

D. A. Reed
University of Tennesse
Knoxville, Tennessee

Abstract

The time-domain current induced in infinitely long, highly conducting, parallel wires above a finitely conducting plane earth in the presence of a plane electromagnetic wave is investigated. The plane wave is assumed to have its magnetic field perpendicular to the axis of the wires, and takes the time-domain form of a double-exponential pulse. Results indicate that the currents are generally smaller than that induced in an isolated conductor because of the coupling between wires and the ground reflection.

*Research reported in this Note was sponsored by the Division of Electric Energy Systems, U.S. Department of Energy, and was performed at the Oak Ridge National Laboratory under Contract No. DE-AC05-840R21400 with Martin Marietta Energy Systems, Inc.

I. INTRODUCTION

When infinitely-long, parallel, highly-conducting wires over a flat earth are exposed to plane-wave excitation, many scattered or reflected waves contribute to the currents induced in the wires. When the "boundary-value problem" approach is taken, it is extremely difficult to obtain useful results unless the less significant waves are ignored. After demonstrating that these waves can, in fact, be ignored for present purposes, the time-domain current induced in the wires can be obtained from the usual phasor forms by numerical inversion of the Fourier transform. In general, the parameters are wire radii, angle of arrival of the plane wave, height of the wires, spacing between wires, ground conductivity, and ground permittivity. The plane wave takes the usual form of a double-exponential pulse.

II. PERFECTLY CONDUCTING WIRE OVER A PERFECTLY CONDUCTING FLAT EARTH

Consider first the case of a single perfectly conducting wire of radius a meters whose axis is h_1 meters above the perfectly conducting ground plane as shown in Figure 1. This boundary value problem has been solved[1], and its solution is expedited by Graf's addition theorem[2] for Bessel functions and the Wronskian for Bessel functions. The need for the Wronskian arises in almost all boundary value problems with cylindrical surfaces, while the addition theorem is needed here to express cylindrical wave functions centered on one axis in terms of cylindrical wave functions arising from another axis. There are three waves that are incident on the cylinder: (1) the given incident plane wave, (2) the plane wave reflected from the ground plane, and (3) the cylindrical wave scattered from the cylinder, reflected from the ground plane, and incident again on the cylinder (that requires Graf's addition theorem). In the interest of brevity only the principal results will be presented.

The axial current induced in the cylinder is given exactly by

$$I_z(\omega) = -\frac{4\,E_o(\omega)}{\mu_o \omega \sin\theta}\, e^{-jk_z z}\, \frac{a_o}{J_o(k_\rho a)} \qquad (1)$$

where

$E_o(\omega)$ = phasor electric field of the incident field

$\mu_o = 4\pi \times 10^{-7}$

$\varepsilon_o = 10^{-9}/36\pi$

$k_\rho = \omega\sqrt{\mu_o \varepsilon_o}\,\sin\theta$

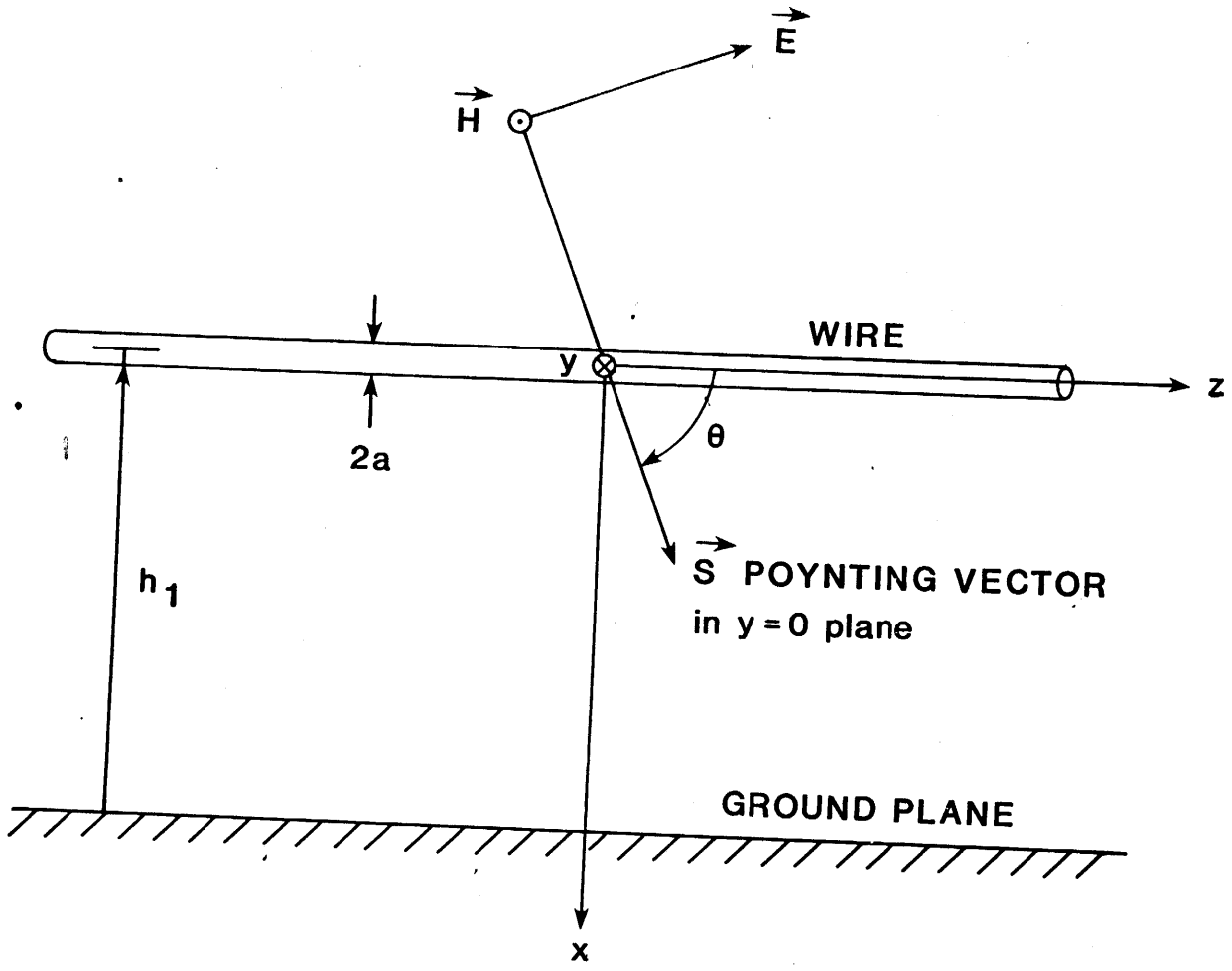
E
H
WIRE
y
z
2a
θ
h 1
S POYNTING VECTOR
in y = 0 plane
GROUND PLANE
x

$$k_z = \omega\sqrt{\mu_o \varepsilon_o}\cos\theta$$

$J_o(x)$ = Bessel function, first kind, order zero

When boundary conditions on tangential E are satisfied at the wire and the ground plane, a_0 is found from

$$0 = (j^{-n} - j^n e^{-j2k_\rho h_1})\frac{J_n(k_\rho a)}{H_n^{(2)}(k_\rho a)} + a_n - \frac{J_n(k_\rho a)}{H_n^{(2)}(k_\rho a)} \sum_{p=-\infty}^{\infty} a_p H_{p+n}^{(2)}(2k_\rho h_1) \qquad (2)$$

where

$H_n^{(2)}(x)$ = Hankel function, second kind, order n, or outward cylindrical wave function.

Equation (2) has the matrix form

$$0 = e + a - b\,a \qquad (3)$$

whose formal solution is

$$a = (b - 1)^{-1} e \qquad (4)$$

On the other hand, the third term in (2) is due to the field that is scattered from the cylinder, reflected from the ground, and incident again on the cylinder. It will normally be small. For $k_\rho a << 1$ the leading term in the series is dominant, and if all higher order terms are ignored, then it is easy to solve for a_0 in (2):

$$a_0 \approx \frac{(1 - e^{-j2k_\rho h_1})J_o(k_\rho a)}{H_o^{(2)}(k_\rho a) - J_o(k_\rho a)H_o^{(2)}(2k_\rho h_1)} \qquad (5)$$

Thus,

$$I_z(\omega) \approx \frac{4E_o(\omega)}{\mu_o \omega \sin\theta} e^{-jk_z z} \frac{1 - e^{-j2k_\rho h_1}}{H_o^{(2)}(k_\rho a) - J_o(k_\rho a)H_o^{(2)}(2k_\rho h_1)} \qquad (6)$$

This is the Flammer-Singhaus[1] result. Since it has already been assumed that $k_\rho a << 1$, then $J_o(k_\rho a) \approx 1$ and (6) further simplifies to

$$I_z(\omega) \approx \frac{4\,E_0(\omega)}{\mu_0 \omega \sin\theta}\, e^{-jk_z z}\, \frac{1 - e^{-j2k_\rho h_1}}{H_0^{(2)}(k_\rho a) - J_0(k_\rho a) H_0^{(2)}(2k_\rho h_1)}$$

For an isolated perfect conductor (1) still applies, but

$$a_0 = -\frac{J_0(k_\rho a)}{H_0^{(2)}(k_\rho a)} \tag{7}$$

so, the (exact) current is

$$I_z(\omega) = \frac{4\,E_0(\omega)}{\mu_0 \omega \sin\theta}\, e^{-jk_z z}\, \frac{1}{H_0^{(2)}(k_\rho a)} \tag{8}$$

A comparison of (6) and (8) [less the phase factor in (6)] is shown in Figure (2) where the effect of the second term in the denominator of (6) can be seen. The magnitude plots are in decibels, where $dB = 20 \log_{10}|I_z(\omega)|$, ignoring the term $1\text{-}\exp(-j2k_\rho h_1)$ in (6).

Equation (8) can be written

$$I_z(\omega) = \left| \frac{4\, e^{-jk_z z}}{\mu_0 \omega \sin\theta} \right| \left| \frac{1}{H_0^{(2)}(k_\rho a)} \right| \left| E_0(\omega) \right|$$

or

$$I_z(\omega) = G_1(\omega)\, G_2(\omega)\, E_0(\omega) \tag{9}$$

In the same way, if $H(\omega) \equiv J_0(k_\rho a) H_0^{(2)}(2k_\rho h_1)$, (6) can be written

$$I_z(\omega) = G_1(\omega)\, \frac{G_2(\omega)}{1 - G_2(\omega) H(\omega)}\, E_0(\omega)$$

$$- e^{-2k_\rho h_1} G_1(\omega)\, \frac{G_2(\omega)}{1 - G_2(\omega) H(\omega)}\, E_0(\omega) \tag{10}$$

Equations (9) and (10) have the block diagram representations shown in Figures 3. It is interesting to observe that the effects of the three "incident waves" mentioned in the first paragraph can be identified as signals appearing at the summation point in Figure 3(b) from:

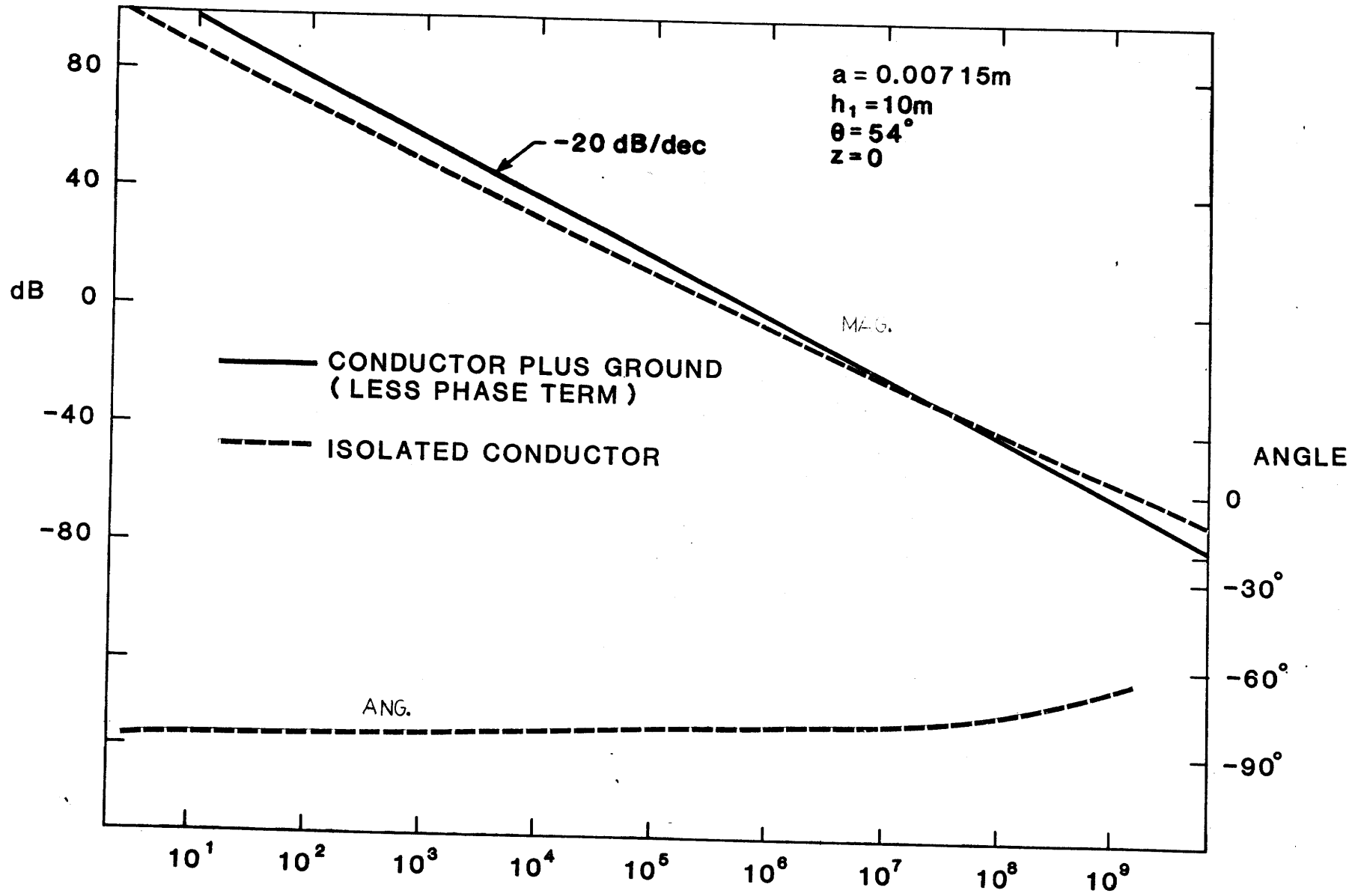

Figure 2. A comparison of the induced current in a conductor above ground (less the phase factor in the numerator) (6) to that in an isolated conductor (8).

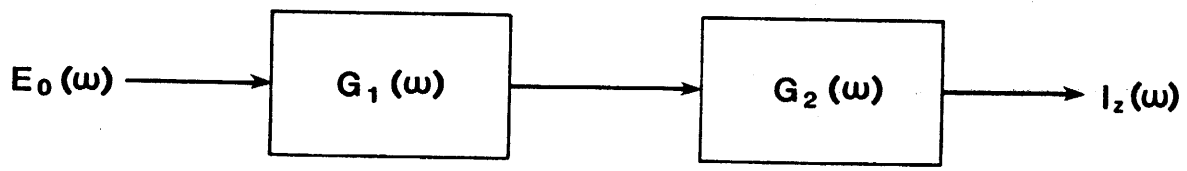

(a)

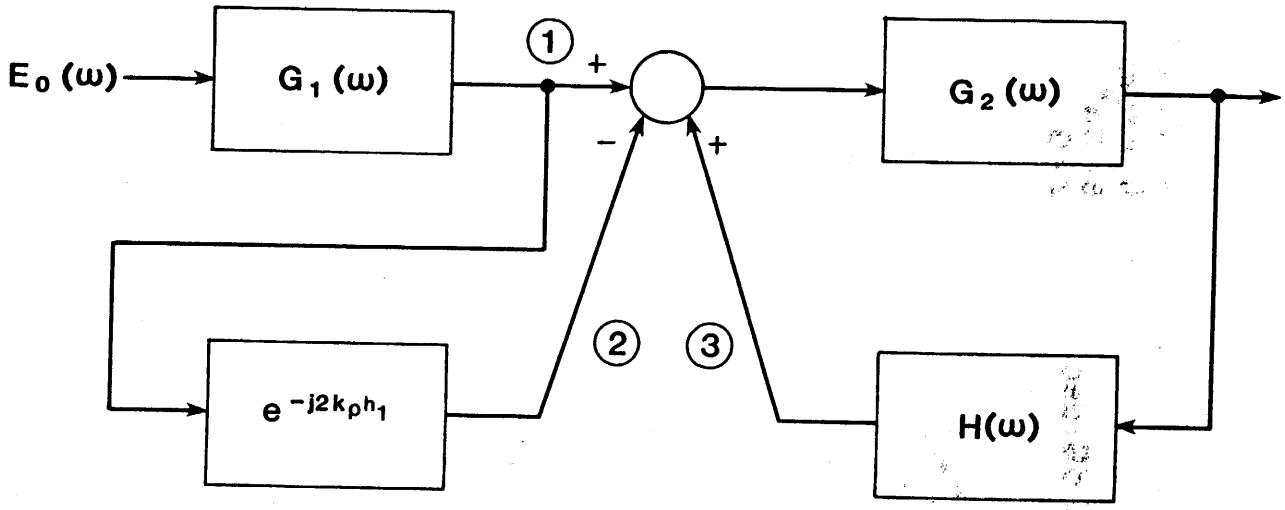

(b)

Figure 3. Block diagram representation of the one-conductor system. (a) Without the ground plane. (b) With the ground plane.

(1) the direct plane wave,

(2) the plane wave reflected from the ground plane, and

(3) the cylindrical wave scattered from the cylinder and reflected from the ground plane back (feedback) to the cylinder.

For $2k_\rho h_1 < 1$ and $k_\rho a < 1$ (that is, for low and intermediate frequencies)

$$J_0(k_\rho a) \approx 1$$

$$H_0^{(2)}(k_\rho a) \approx 1 - j\frac{2}{\pi}\ell n(\gamma k_\rho a/2)$$

$$H_0^{(2)}(2k_\rho h_1) \approx 1 - j\frac{2}{\pi}\ell n(\gamma k_\rho h_1)$$

$$= 1.781$$

With these approximations (6) becomes ($z = 0$):

$$I_z(\omega) \approx \frac{5 \times 10^9}{\sin\theta\, \ell n(2h_1/a)} \frac{E_0(\omega)}{j\omega}\left(1 - e^{-j2k_\rho h_1}\right) \tag{11}$$

It is often assumed that the plane wave from an electromagnetic pulse has the form

$$E_0(t) = E_0(e^{-a_1 t} - e^{-a_2 t})u(t)$$

Therefore

$$E_0(\omega) = E_0\left(\frac{1}{j\omega + a_1} - \frac{1}{j\omega + a_2}\right)$$

and then $i_z(t)$ is particularly easy to find by inversion. Using typical values:

$a = 0.00715$ m

$h_1 = 10$ m

$\theta = 54°$

$$E_o = 52{,}500 \text{ v/m}$$

$$\alpha_1 = 4 \times 10^6 s^{-1}$$

$$\alpha_2 = 478 \times 10^6 s^{-1}$$

$$i_z(t) \approx 10{,}136 \left\{ \left| 1 - \frac{478}{474} e^{-4 \times 10^6 t} + \frac{4}{474} e^{-478 \times 10^6 t} \right| u(t) \right.$$

$$\left. - \left| 1 - \frac{478}{474} e^{-4 \times 10^6 (t - t_o)} + \frac{4}{474} e^{-478 \times 10^6 (t - t_o)} \right| u(t - t_o) \right\} \qquad (12)$$

where $t_o = 2h_1 \sin\theta / c$. Results are shown in Figure 4 along with those for the same conductor with no ground plane from Barnes[3]. Notice the reduction in peak current.

Since it has already been assumed that $k_\rho h_1 << 1$,

$$1 - e^{-j2k_\rho h_1} \approx j2k_\rho h_1$$

Using this approximation in (11) gives

$$I_z(\omega) \approx \frac{2 E_o(\omega) h_1}{(\eta_o / 2\pi) \ell n(2h_1/a)} e^{-jk_z z}$$

but since the characteristic impedance of a single wire over a perfect ground (TEM mode) is given approximately ($h_1 >> a$) by

$$Z_o \approx \frac{\eta_o}{2\pi} \ell n(2h_1/a)$$

$$I_z(\omega) \approx \frac{2 E_o(\omega) h_1}{Z_o} e^{-jk_z z} \qquad (13)$$

The time-domain result ($z = 0$) is

$$I_z(t) \approx \frac{2 E_o h_1}{Z_o} \left(e^{-\alpha_1 t} - e^{-\alpha_2 t} \right) u(t) \qquad (14)$$

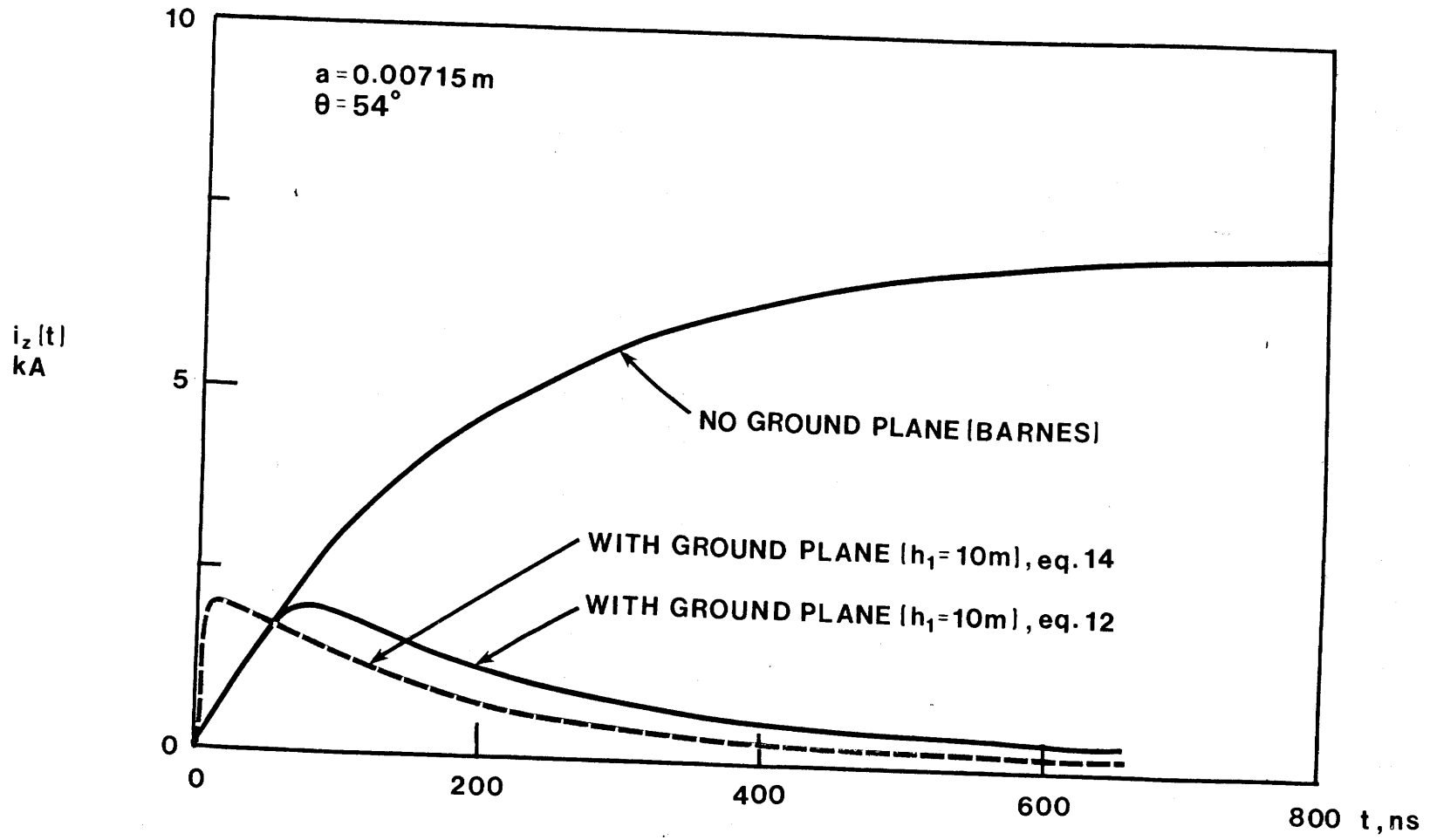

Figure 4. A comparison of the induced currents: with and without a perfectly conducting ground plane (θ = 54°, a = 0.00715 m).

and is shown in Figure 4 for comparison with (12). Results indicate that (11) [leading to (12)] gives good results for early time, whereas (13) [leading to (14)] does not. The reason for this is obvious. The approximation above (13) not only eliminated the time delay for the ground reflected wave in (11), but in so doing it canceled the $j\omega$ in the denominator in (11). This enhances the high-frequency or early-time response, as Figure 4 shows.

The differential equations describing a single wire over ground subject to emp can be written so as to incorporate the emp in terms of induced voltages and currents per unit length[4]:

$$\frac{dV_z}{dz} + ZI_z = V_z' \tag{15}$$

$$\frac{dI_z}{dz} + Y V_z = I_z' \tag{16}$$

When the proper forms for V'_z and I'_z are used, and (15) and (16) are uncoupled, the result for I_z is the same as (11). Thus it can be concluded that for low and intermediate frequency the exact result given by (1) reduces to the transmission line result given by (11).

III. MULTIPLE PERFECTLY CONDUCTING WIRES OVER A PERFECTLY CONDUCTING FLAT EARTH

Having seen the approximation that was necessary (and valid) to avoid an infinite series in the expression for the induced current in the single wire (above ground) case, the same approximations can be made in order to obtain the current for the case of multiple parallel wires above ground. Consider, as an example, four wires. The geometry is shown in Figure 5. Keeping only the leading terms in the series expressions for the scattered fields (that is, the Hankel functions), and satisfying boundary conditions at the four conductor surfaces and the ground plane, leads to four equations in four unknowns:

$$-2j\sin(k_\rho h_1)e^{-jk_\rho h_1} = a_0 h_{11} + b_0 h_{12} + c_0 h_{13} + d_0 h_{14}$$

$$-2j\sin(k_\rho h_1)e^{-jk_\rho h_1} = a_0 h_{12} + b_0 h_{22} + c_0 h_{23} + d_0 h_{24} \qquad (17)$$

$$-2j\sin(k_\rho h_1)e^{-jk_\rho h_1} = a_0 h_{13} + b_0 h_{23} + c_0 h_{33} + d_0 h_{34}$$

$$-2j\sin(k_\rho h_1)e^{-jk_\rho h_1} = a_0 h_{14} + b_0 h_{24} + c_0 h_{34} + d_0 h_{44}$$

where

$$h_{11} = \frac{H_0^{(2)}(k_\rho a)}{J_0(k_\rho a)} - H_0^{(2)}(2k_\rho h_1)$$

$$h_{12} = H_0^{(2)}(k_\rho \rho_{12}) - H_0^{(2)}(k_\rho \rho'_{12})$$

$$h_{13} = H_0^{(2)}(k_\rho \rho_{13}) - H_0^{(2)}(k_\rho \rho'_{13})$$

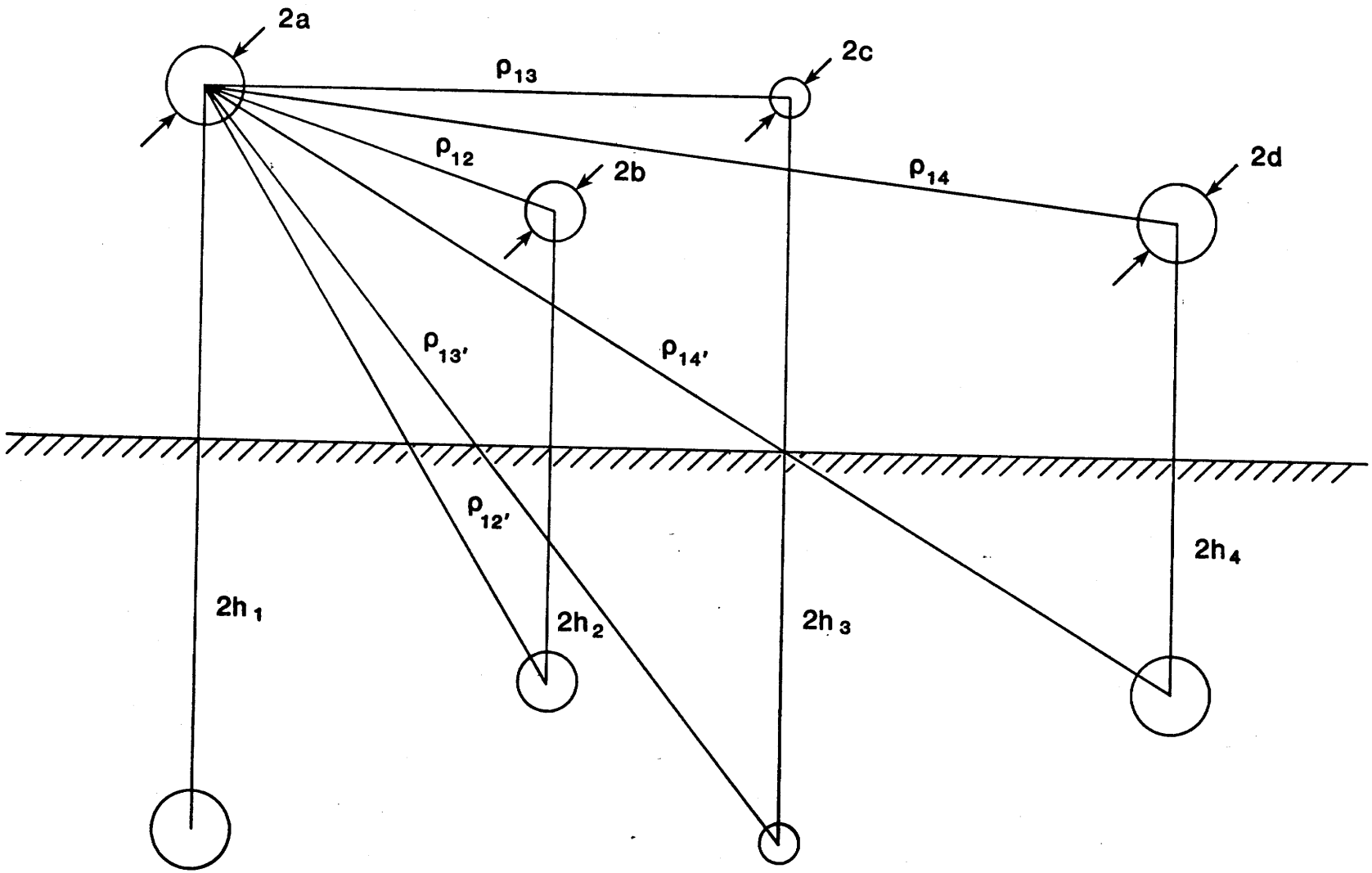

Figure 5. Geometry for four conductors (and their images) with a ground plane.

$$h_{14} = H_0^{(2)}(k_\rho \rho_{14}) - H_0^{(2)}(k_\rho \rho'_{14})$$

$$h_{22} = \frac{H_0^{(2)}(k_\rho b)}{J_0(k_\rho b)} - H_0^{(2)}(2k_\rho h_2)$$

$$h_{23} = H_0^{(2)}(k_\rho \rho_{23}) - H_0^{(2)}(k_\rho \rho'_{23})$$

etc.

The axial current in the cylinders has the same <u>form</u> as that for a single wire (1):

$$I_{za}(\omega) \approx -\frac{4E_o(\omega)}{\mu_0 \omega \sin\theta} e^{-jk_z z} \frac{a_o}{J_o(k_\rho a)} \tag{18}$$

for the cylinder $\rho = a$. For the cylinder $\rho = b$:

$$I_{zb}(\omega) \approx -\frac{4E_o(\omega)}{\mu_0 \omega \sin\theta} e^{-jk_z z} \frac{b_o}{J_o(k_\rho b)} \tag{19}$$

etc. Thus, the set (17) must be solved in order to find the current.

If the wire spacing is very large such that $k_\rho \rho'_{mn} >> 1$, then $h_{mn} \approx 0$, $m \neq n$, and (18) becomes identical to (6) as it should. Also, if there is no ground plane, then (17) becomes

$$-1 = a_0 h_{11} + b_0 h_{12} + c_0 h_{13} + d_0 h_{14}$$

$$-e^{-jk_\rho (h_1 - h_2)} = a_0 h_{12} + b_0 h_{22} + c_o h_{23} + d_0 h_{24} \tag{20}$$

$$-e^{-jk_\rho (h_1 - h_3)} = a_0 h_{13} + b_0 h_{23} + c_o h_{33} + d_0 h_{34}$$

$$-e^{-jk_\rho (h_1 - h_4)} = a_0 h_{14} + b_0 h_{24} + c_o h_{34} + d_0 h_{44}$$

where

$$h_{11} = \frac{H_0^{(2)}(k_\rho a)}{J_0(k_\rho a)}, \; h_{22} = \frac{H_0^{(2)}(k_\rho b)}{J_0(k_\rho b)}, \text{ etc.}$$

$$h_{12} = H_0^{(2)}(k_\rho \rho_{12}), \; h_{13} = H_0^{(2)}(k_\rho \rho_{13}), \text{ etc.}$$

and I_{za} is still given by (1).

For two conductors and a ground plane it is not difficult to solve for a_0, b_0, I_{za}, and I_{zb}. The resulting (coupled) block diagram is shown in Figure 6. In this diagram

$$G_a = \frac{1}{H_0^{(2)}(k_\rho a)} \qquad H_a = J_0(k_\rho a) H_0^{(2)}(2k_\rho h_1) \tag{21}$$

$$G_b = \frac{1}{H_0^{(2)}(k_\rho a)} \qquad H_b = J_0(k_\rho b) H_0^{(2)}(2k_\rho h_1) \tag{22}$$

$$G_{a1} = J_0(k_\rho a) H_0^{(2)}(k_\rho \rho_{12}) \qquad G_{b1} = J_0(k_\rho b) H_0^{(2)}(k_\rho \rho_{12}) \tag{23}$$

$$G_{a1} = J_0(k_\rho a) H_0^{(2)}(k_\rho \rho_{12}) \qquad G_{b1} = J_0(k_\rho b) H_0^{(2)}(k_\rho \rho_{12}) \tag{24}$$

The various contributions to each current can be identified in the figure. The signals appearing at the upper summation point are from:

(1) the direct plane wave,

(2) the plane wave reflected from the ground,

(3) the cylindrical wave scattered from cylinder a and reflected from the ground back (feedback) to cylinder a,

(4) the cylindrical wave scattered from cylinder b and directly incident on (coupled to) cylinder a, and

(5) the cylindrical wave scattered from cylinder b, reflected from the ground, and incident on (coupled to) cylinder a.

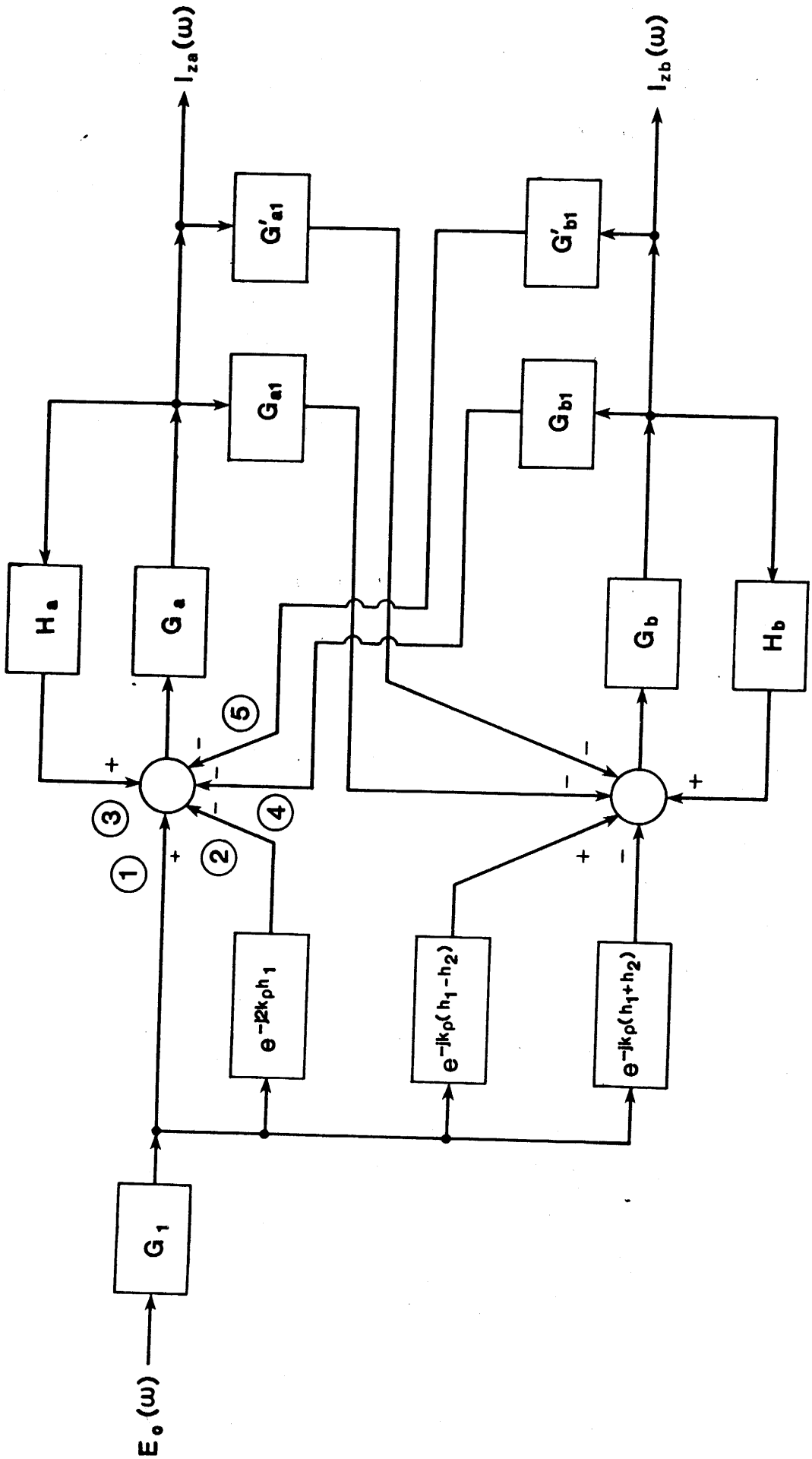

Figure 6. Block diagram for two conductors and a ground plane.

It is helpful to observe the geometry of Figure 5 (conductors a and b only) in conjunction with Figure 6. The currents are obtained from (18 and (19) using (17) (appropriately reduced for the case of two conductors). The currents can also be obtained from the block diagram of Figure 6.

IV. THE EFFECT OF A FINITELY CONDUCTING GROUND

It has been established by several investigators (including the authors of this report-in two separate reports[5,6]) that the finite conductivity of the wires has negligible effect on the early-time behavior of the current induced in an isolated wire for the types of electromagnetic pulses expected [see below (11)]. On the other hand, the effect of a finitely conducting ground ($\sigma < \infty, \varepsilon > \varepsilon_0$) is much more pronounced, and must be considered. This means that the preceding results are only valid for low and (or) intermediate frequencies, whereas early-time behavior is governed by high frequency behavior. Thus, those results are of limited usefulness for present purposes.

It is relatively easy to show, and intuitively obvious, that for high frequencies, two of the waves incident on cylinder a in Figure 5 are small and can be neglected. These are the wave scattered from cylinder a and reflected from the ground back to cylinder a (3), and the cylindrical wave scattered from cylinder b, reflected from the ground, and incident on cylinder a (5). It is expected that these terms are even smaller, and can be neglected when the ground is finitely conducting. It will be demonstrated that this is the case.

Olsen and Chang[7] have derived a formula for the electric field parallel to and resulting from the current of a Hertzian dipole that is parallel to and located h_1 meters above a finitely conducting earth. Thus, this electric field is the "impulse response", and the electric field, E_z, can be found for any z-directed axial filamentary current by convolution:

$$E_z = -j\frac{30}{k}\int_{-\infty}^{\infty} I(z')K(z-z')dz'$$

$$E_z = -j\frac{30}{k}\int_{-\infty}^{\infty} I(z-z')K(z')dz' \qquad (25)$$

For present purposes E_z is to be calculated at the wire (essentially filamentary for $k_\rho\, a << 1$) surface. In this case (see Figure 1) Olsen and Chang give

$$K(z) = k^2(G_{11}-G_{12}+2\,kQ) + \frac{\partial^2}{\partial z^2}(G_{11}-G_{12}+2\,kQ) \qquad (26)$$

where

$$G_{11} = \frac{e^{-jk\sqrt{z^2+a^2}}}{\sqrt{z^2+a^2}}$$

$$G_{12} = \frac{e^{-jk\sqrt{z^2+(2h_1)^2}}}{\sqrt{z^2+(2h_1)^2}} \qquad (h_1 >> a)$$

$$P = \int_0^\infty \frac{1}{\sqrt{\alpha^2-n^2}+n^2\sqrt{\alpha^2-1}}\, e^{-k\sqrt{\alpha^2-1}(2h_1)} J_0(kz\alpha)\alpha\, d\alpha$$

$$Q = \int_0^\infty \frac{1}{\sqrt{\alpha^2-1}+\sqrt{\alpha^2-n^2}}\, e^{-k\sqrt{\alpha^2-1}(2h_1)} J_0(kz\alpha)\alpha\, d\alpha$$

$$n^2 = \varepsilon_R + \frac{\sigma}{j\omega\varepsilon_0} \qquad (\sigma, \varepsilon_R \text{ assumed constant})$$

Because of the nature of the plane wave source, I(z) must be of the form

$$I(z) = I_0 e^{-jk_z z} \qquad (k_z = k\cos(0))$$

so

$$E_z = -j\frac{30}{k} I_0 e^{-jk_z z}\int_{-z}^{z} K(z')\, e^{jk_z z'}\, dz' \qquad (27)$$

The integral in (27) is recognized as the Fourier transform of K(z) evaluated at

$-k_z$ where k_z is the transform variable. That is

$$E_z = -j\frac{30}{k} I_o e^{-jk_z z} \bar{K}(-k_z) \tag{28}$$

where the bar indicates the transformed quantity. The normalized field is

$$E_{zn} = \frac{E_z}{-j\frac{30}{k} I_o e^{-jk_z z}} = \bar{K}(-k_z) \tag{29}$$

Transforming (26) with the aid of a table of pairs gives

$$E_{zn} = -j\pi \sin^2\theta\, H_o^{(2)}(k_\rho a) + j\pi \sin^2\theta\, H_o^{(2)}(2k_\rho h_1)$$

$$+ 4\int_{\cos\theta}^{\infty} \frac{e^{-k\sqrt{\alpha^2-1}(2h_1)}}{\sqrt{\alpha^2-n^2}+\sqrt{\alpha^2-1}} \cdot \frac{\alpha}{\sqrt{\alpha^2-\cos^2\theta}}\, d\alpha$$

$$+ 4\cos^2\theta\int_{\cos\theta}^{\infty} \frac{e^{-k\sqrt{\alpha^2-1}(2h_1)}}{\sqrt{\alpha^2-n^2}+\sqrt{\alpha^2-1}} \cdot \frac{\alpha}{\sqrt{\alpha^2-\cos^2\theta}}\, d\alpha \tag{30}$$

or

$$E_{zn} \equiv E_1 + E_2 + E_3 + E_4 \tag{31}$$

The first term in (30 or (31) is recognized as the normalized field due to the current with no ground present. Then the last three terms in (30) must be the field scattered from the finitely conducting ground ($\sigma, \varepsilon = \varepsilon_R \varepsilon_0$). The ratio $|E2 + E3 + E4|/|E1|$ is the ratio of the magnitude of the field at the wire that is scattered from the ground to the magnitude of the field at the wire produced directly by the current. This ratio in dB* is shown in Figures 7 through 10 plotted against frequency for $\omega = 10$ to 10^9 for various ground constants and values of θ. Notice that, as expected, this ratio is quite small for high frequencies, incicating that for early-time behavior (only) cylindrical waves arising from the wires and scattered from the ground can be safely neglected.

*$20 \log_{10}\left|\frac{E_2+E_3+E_4}{E_1}\right|$. The curves for θ = 54°, 36°, 18° and 6° are referenced to the curve for θ = 90° at ω = 10.

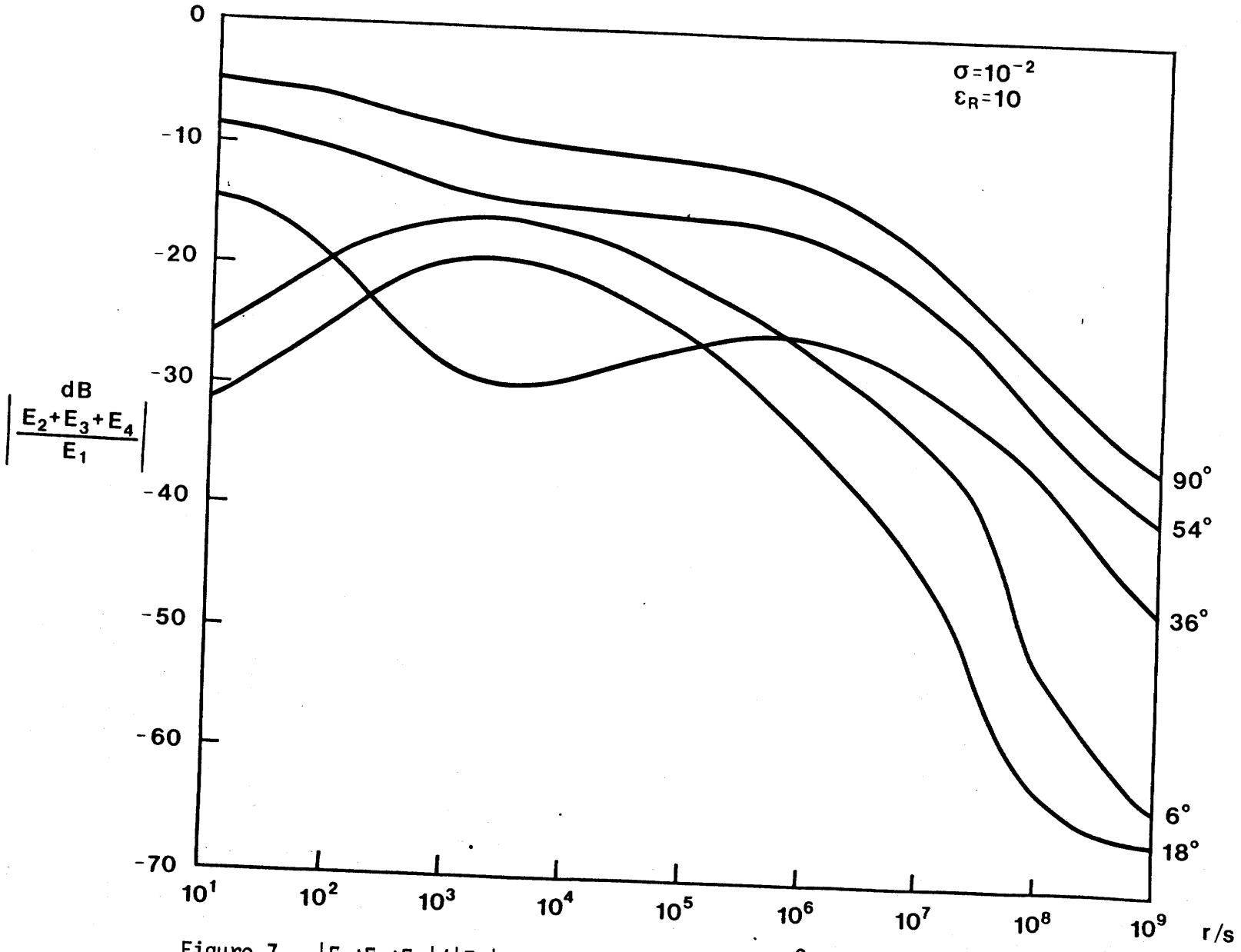

Figure 7. $|E_2+E_3+E_4|/|E_1|$ in dB versus ω: $\sigma = 10^{-2}$, $\varepsilon_R = 10$. The angle θ is the parameter.

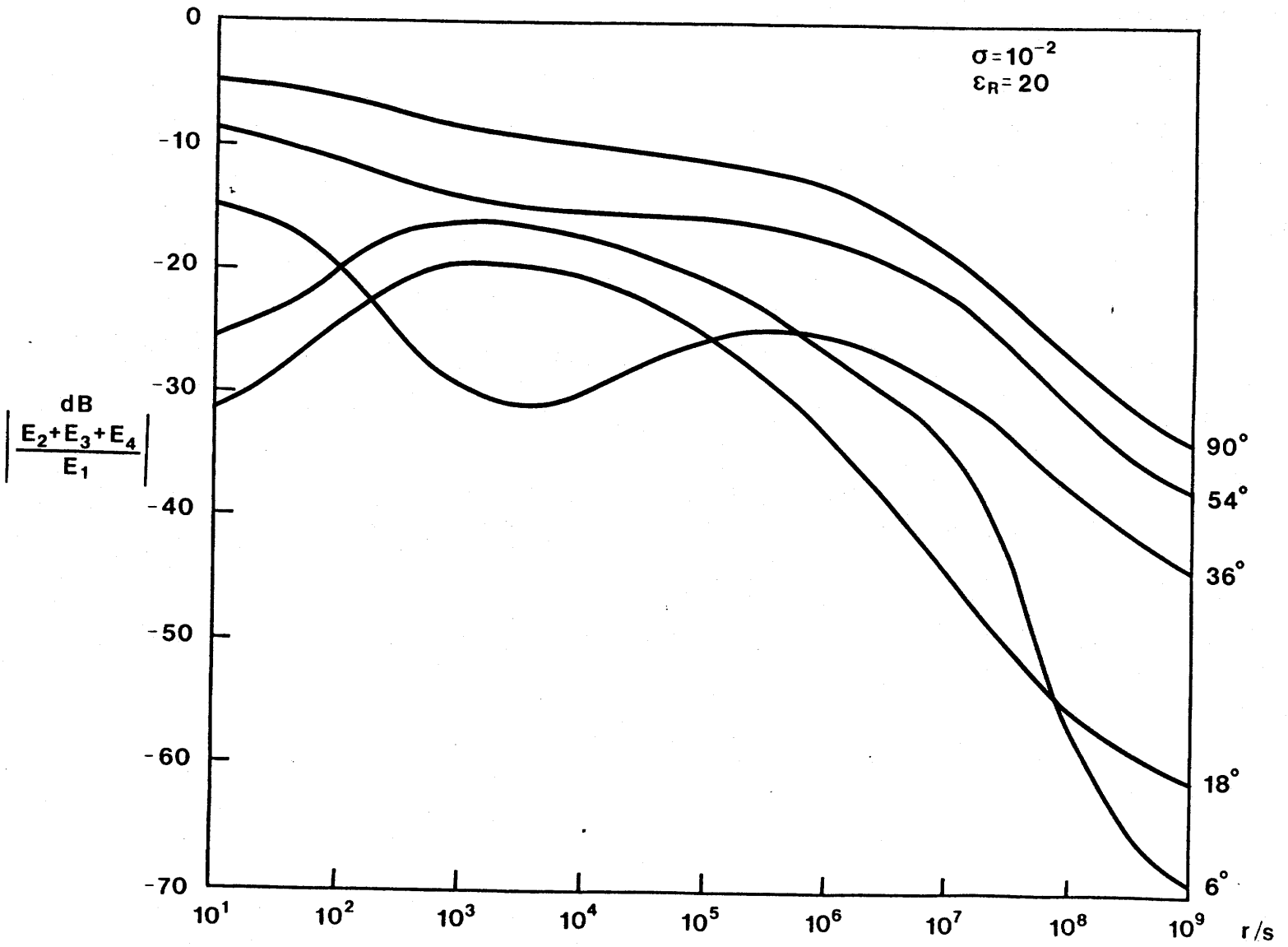

Figure 8. $|E_2+E_3+E_4|/|E_1|$ in dB versus ω: $\sigma = 10^{-2}$, $\varepsilon_R = 20$. The angle θ is the parameter.

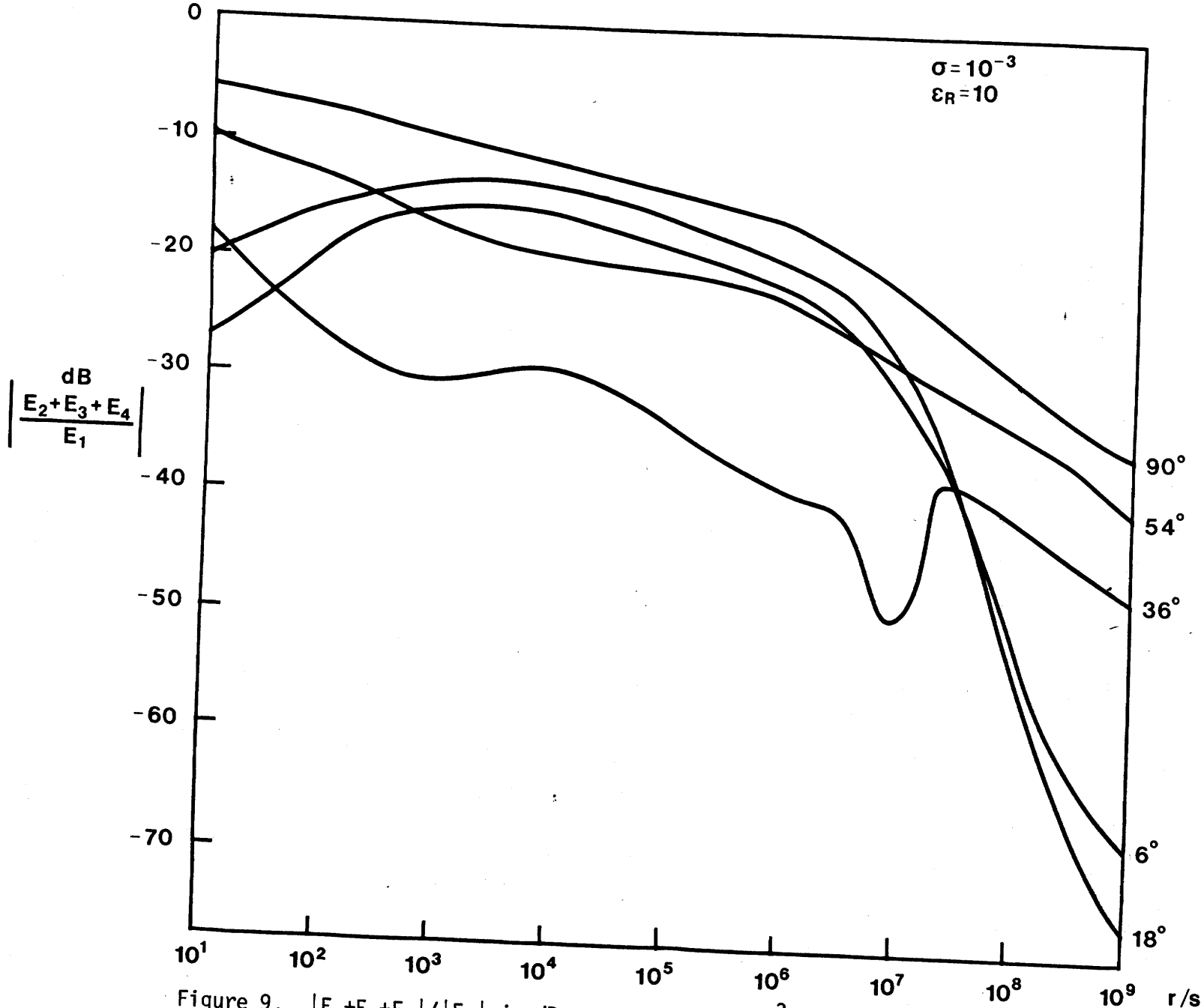

Figure 9. $|E_2+E_3+E_4|/|E_1|$ in dB versus ω: $\sigma = 10^{-3}$, $\varepsilon_R = 10$. The angle θ is the parameter.

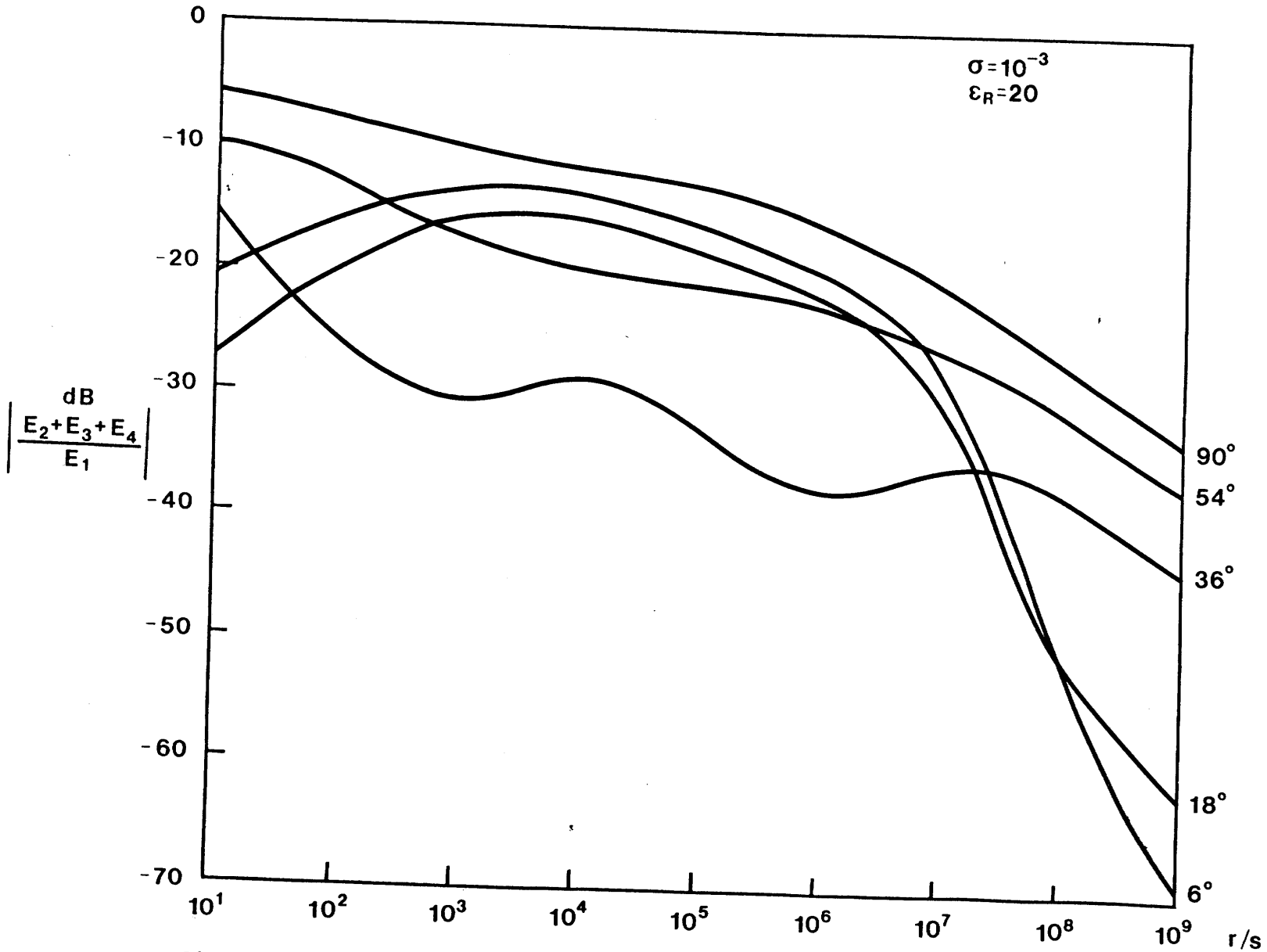

Figure 10. $|E_2+E_3+E_4|/|E_1|$ in dB versus ω: $\sigma = 10^{-3}$, $\varepsilon_R = 20$. The angle θ is the parameter.

Thus a reasonable model for a single wire and a finitely conducting ground becomes that shown in Figure 11. It should be compared to Figure 3(b). The current is given by

$$I_z(\omega) = \frac{4\,E_o(\omega)}{\mu_o \omega \sin\theta}\, e^{-jk_z z}\, \frac{1 + \Gamma_H(\omega)\, e^{-j2k_\rho h_1}}{H_o^{(2)}(k_\rho a)} \tag{32}$$

where the coefficent of reflection is given by

$$\Gamma_H(\omega) = \frac{E_r(\omega)}{E_i(\omega)} = -\,\frac{1 - \dfrac{1}{\sqrt{\varepsilon_R}\sin\theta}\sqrt{1 - \dfrac{\sigma/\varepsilon}{\sigma/\varepsilon + j\omega}}\sqrt{1 - \dfrac{\cos^2\theta}{\varepsilon_R}\left(1 - \dfrac{\sigma/\varepsilon}{\sigma/\varepsilon + j\omega}\right)}}{1 + \dfrac{1}{\sqrt{\varepsilon_R}\sin\theta}\sqrt{1 - \dfrac{\sigma/\varepsilon}{\sigma/\varepsilon + j\omega}}\sqrt{1 - \dfrac{\cos^2\theta}{\varepsilon_R}\left(1 - \dfrac{\sigma/\varepsilon}{\sigma/\varepsilon + j\omega}\right)}} \tag{33}$$

Using the same approximations once more, the block diagram for two conductors and a finitely conducting ground becomes that shown in Figure 12. See Figure 6 for comparison. When $k_\rho a$ and $k_\rho b$ are small, $G_{a1} \approx G_{a2} \approx H_0^{(2)}(k_\rho \rho_{12})$ from (23). In this case the currents are given by

$$I_{za} = E_o G_1 G_a\, \frac{1 + \Gamma_H e^{-j2k_\rho h_1} - G_b G_{a1}\left[e^{-jk_\rho (h_1 - h_2)} + \Gamma_H e^{-jk_\rho (h_1 + h_2)}\right]}{1 - G_a G_b G_{a1}^2} \tag{34}$$

$$I_{zb} = E_o G_1 G_b\, \frac{\left[e^{-jk_\rho (h_1 - h_2)} + \Gamma_H e^{-jk_\rho (h_1 + h_2)}\right] - G_a G_{a1}\left[1 + \Gamma_H e^{-j2k_\rho h_1}\right]}{1 - G_a G_b G_{a1}^2} \tag{35}$$

where G_1, G_a, and G_b are given by (9), (21), and (22), respectively.

If the case $h_1 = h_2$, $a = b = 0.00715$ m, $\rho_{12} = 9$ m, and $\theta = \pi/2$ is considered, then the ratio of the current given by (34) to that given by (32) is $1/(1 + G_a G_{a1})$, which is less than unity for frequencies up to $\omega \approx 10^8$. This shows that the coupling reduces the induced phasor current.

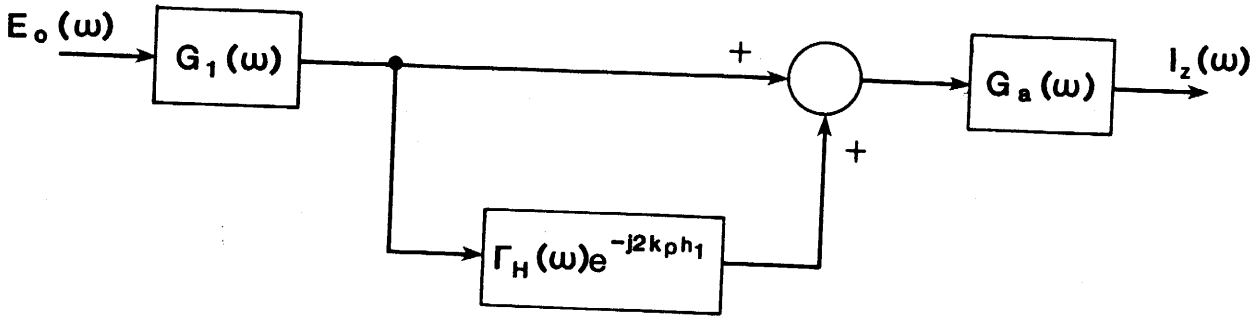

Figure 11. Simplified block diagram representation of the one-conductor system with a finitely conducting ground (ignoring secondary scattering).

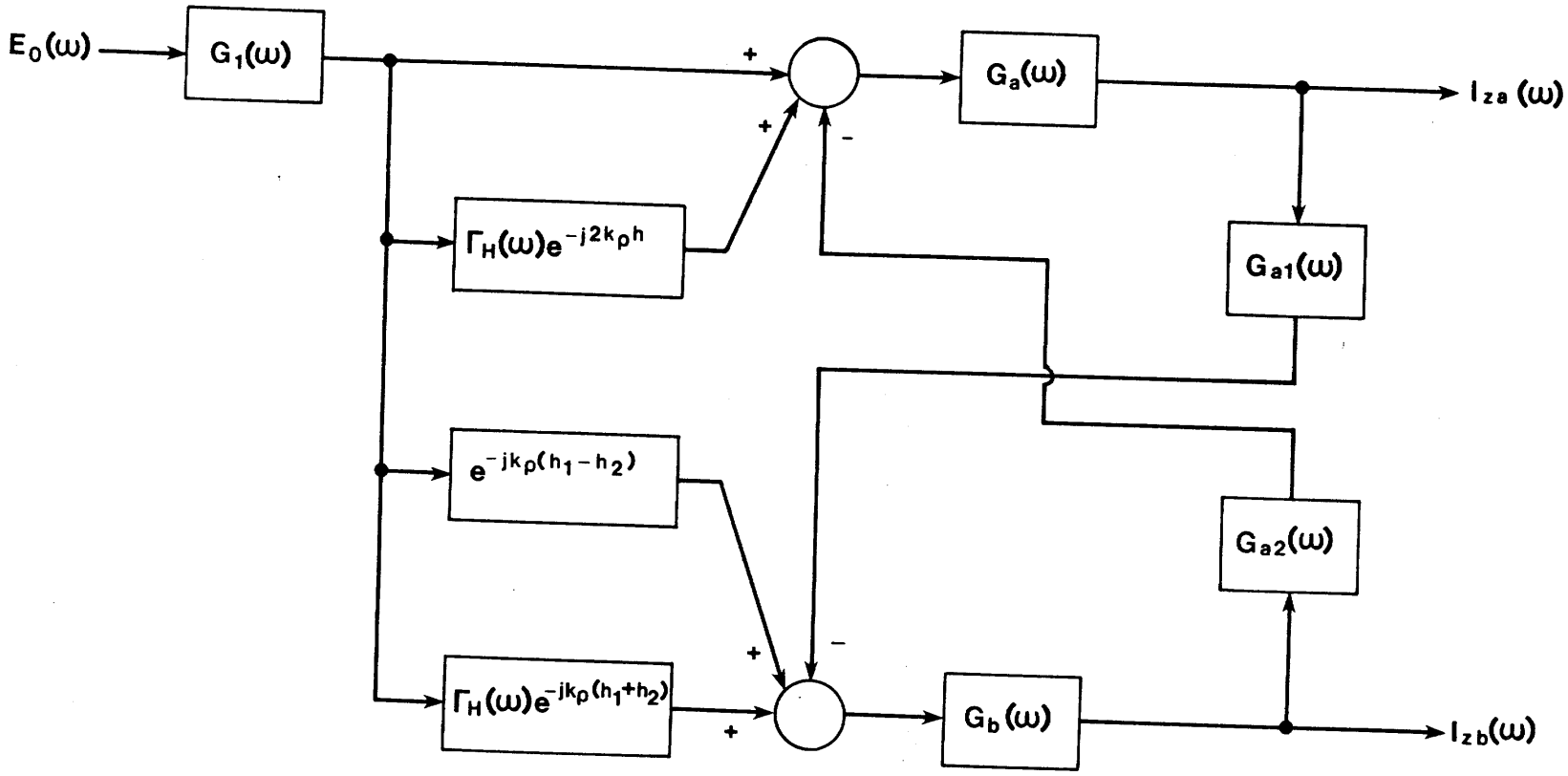

Figure 12. Simplified block diagram representation of the two-conductor system with a finitely conducting ground (ignoring secondary scattering).

Having seen the approximations that are made in order to simplify the two-conductor case, it is a relatively simple matter to extend these to the three or four-conductor case.

The assumption of a thin wire ($k_\rho a << 1$) permits the calculation of the current induced in the wire when over a finitely conducting ground and subject to plane wave excitation. The Olsen and Chang results, however, require infinite integrations (30) for each frequency. Time-domain results, in turn, require another infinite integration (inverse Fourier transform). This is quite a formidable task, and one is willing to use the approximations (above) in order to obtain useful results.

The Brewster angle for Figure 1 is the angle ($\theta = \theta_B$) for which there is no reflection when $\sigma = 0$. It is given by

$$\theta_B = \cos^{-1} \sqrt{\frac{\varepsilon_R}{\varepsilon_R + 1}} \qquad (36)$$

The high-frequency behavior of $\Gamma_H(\omega)$ is of primary concern here. At high frequencies[6], $\omega > 10\,\sigma/\varepsilon$, and $\theta > \theta_B$, the magnitude of Γ_H is constant (< 1), while the phase angle of Γ_H is 180°. For $\omega > 10\,\sigma/\varepsilon$, and $\theta = \theta_B$, the magnitude of Γ_H decreases with ω (20 dB/decade), but its phase angle is exactly 90°. For $\omega > 10\,\sigma/\varepsilon$, and $\theta < \theta_B$, the magnitude of Γ_H is again constant (< 1), but its phase angle is 0°. Thus, a complete phase reversal occurs between the case $\theta > \theta_B$, and $\theta < \theta_B$, and it is to be expected that for angles $\theta < \theta_B$, the reflected wave will enhance, rather than reduce, the early-time current induced in wires above ground by the direct wave. Furthermore, the effect will be more pronounced for smaller ground conductivities, or larger dielectric constants, because the phenomena mentioned above occur at lower frequencies (and extended over a wider band of frequencies). In other words, the relaxation time, ε/σ, is larger.

V. TIME-DOMAIN RESULTS

When secondary scattering is ignored, equation (32) and Figure 11 apply to the case of a single wire over a finitely conducting ground. Time-domain results have been obtained for the double exponential plane wave (described earlier) by numerical inversion of the Fourier transform (32). A wire radius of $a = 0.00715$ m and height $h_1 = 9$ m were used throughout, and the parameter is the angle θ (Figure 1). Four cases (ground conductivity, $\sigma = 10^{-2}$ and 10^{-3}; relative ground permittivity, $\varepsilon_R = 10$ and 15) were considered. The results appear in Figure 13 through 16.

The Brewster angle is $\theta_B = 17.55°$ for $\varepsilon_R = 10$, $\theta_B = 14.48°$ for $\varepsilon_R = 15$. When $\theta > \theta_B$, the ground reflected field reduces the induced current rather quickly, and limits the peak current to approximately 60% of what it would otherwise be at 100 ns. On the other hand, for $\theta < \theta_B$ the reduction is not as great (at 100ns), and, as predicted in Section IV, the ground reflected field may temporarily <u>increase</u> the induced current ($\theta = 10°$); noticeably so for lower ground conductivity.!

Equations (34) and (35) give the induced currents for two wires above ground when secondary scattering is ignored. Figure 12 applies to this case. The same parameters and variables that were mentioned in the first paragraph of this section were used to examine the time-domain behavior of the induced current. In addition, the wires are identical, and $h_1 = h_2 = 9$ m, so that $I_{za} = I_{zb} = I_z$. Results are shown in Figure 17 through 28. The current $i_z(t)$ is the time-domain current induced in either wire. These currents

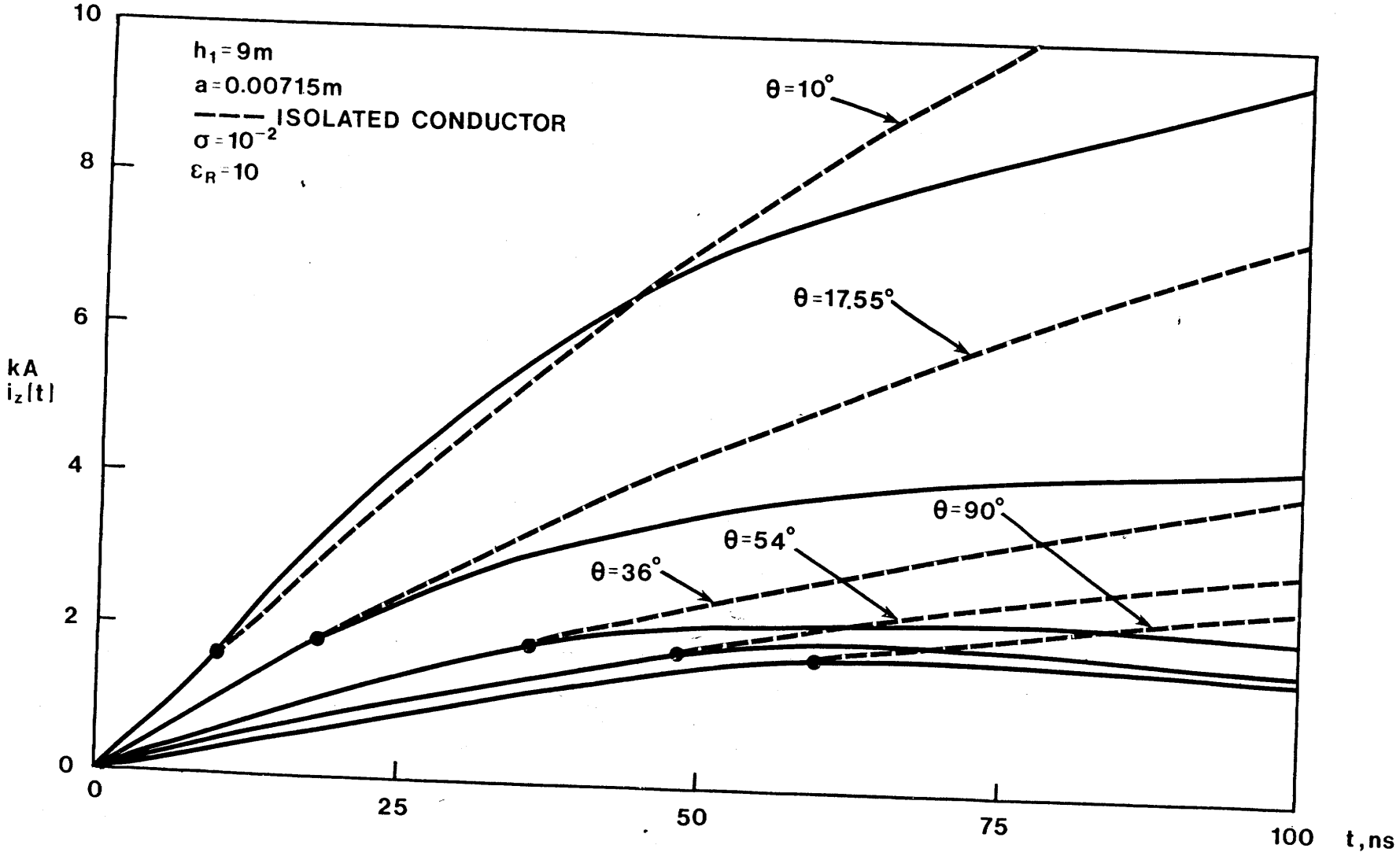

Figure 13. Time-domain current for a single wire above ground: $h_1 = 9m$, $a = 0.00715m$, $\sigma = 10^{-2}$, $\varepsilon_R = 10$.

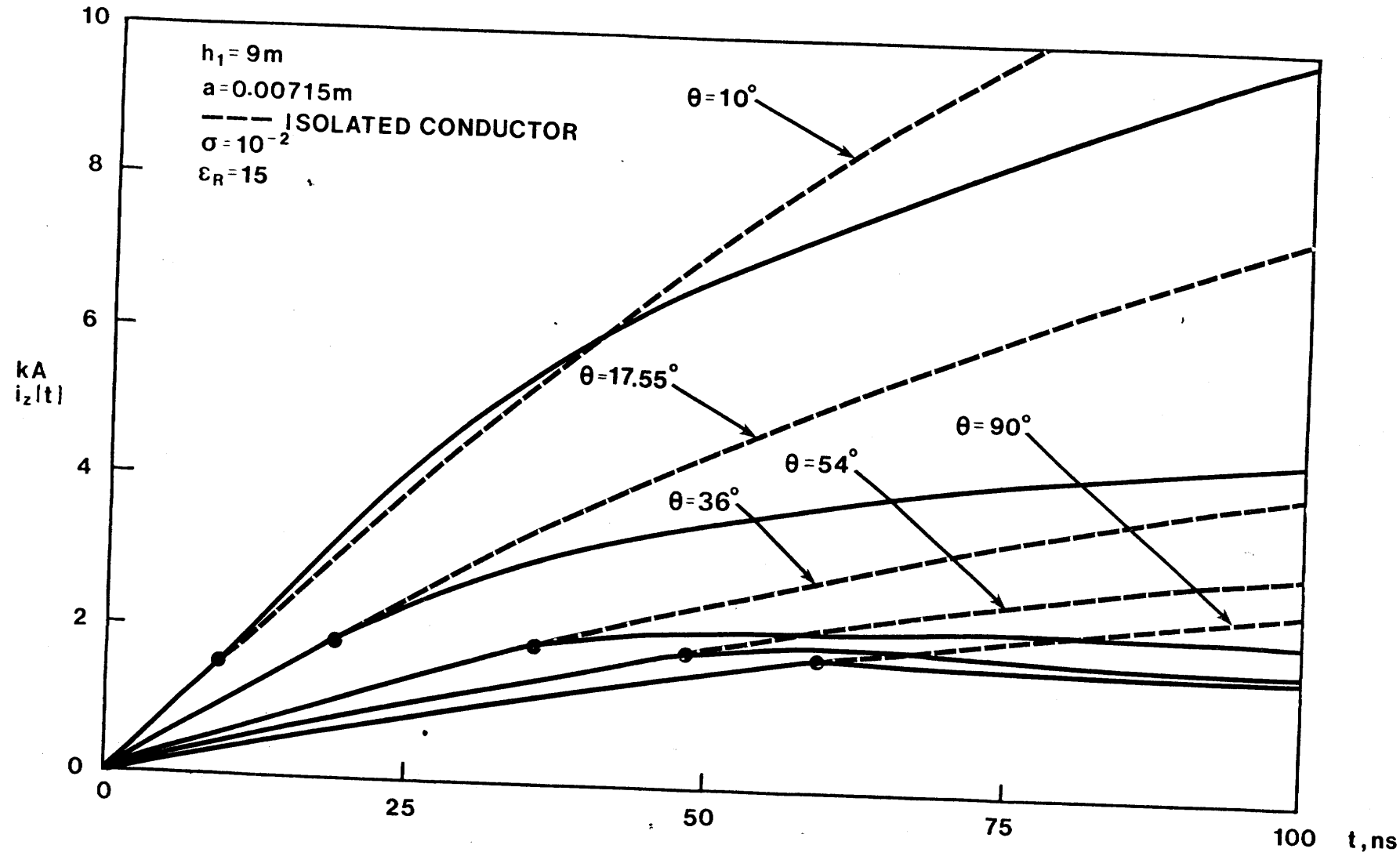

Figure 14. Time-domain current for a single wire above ground: $h_1 = 9m$, $a = 0.00715m$, $\sigma = 10^{-2}$, $\varepsilon_R = 15$.

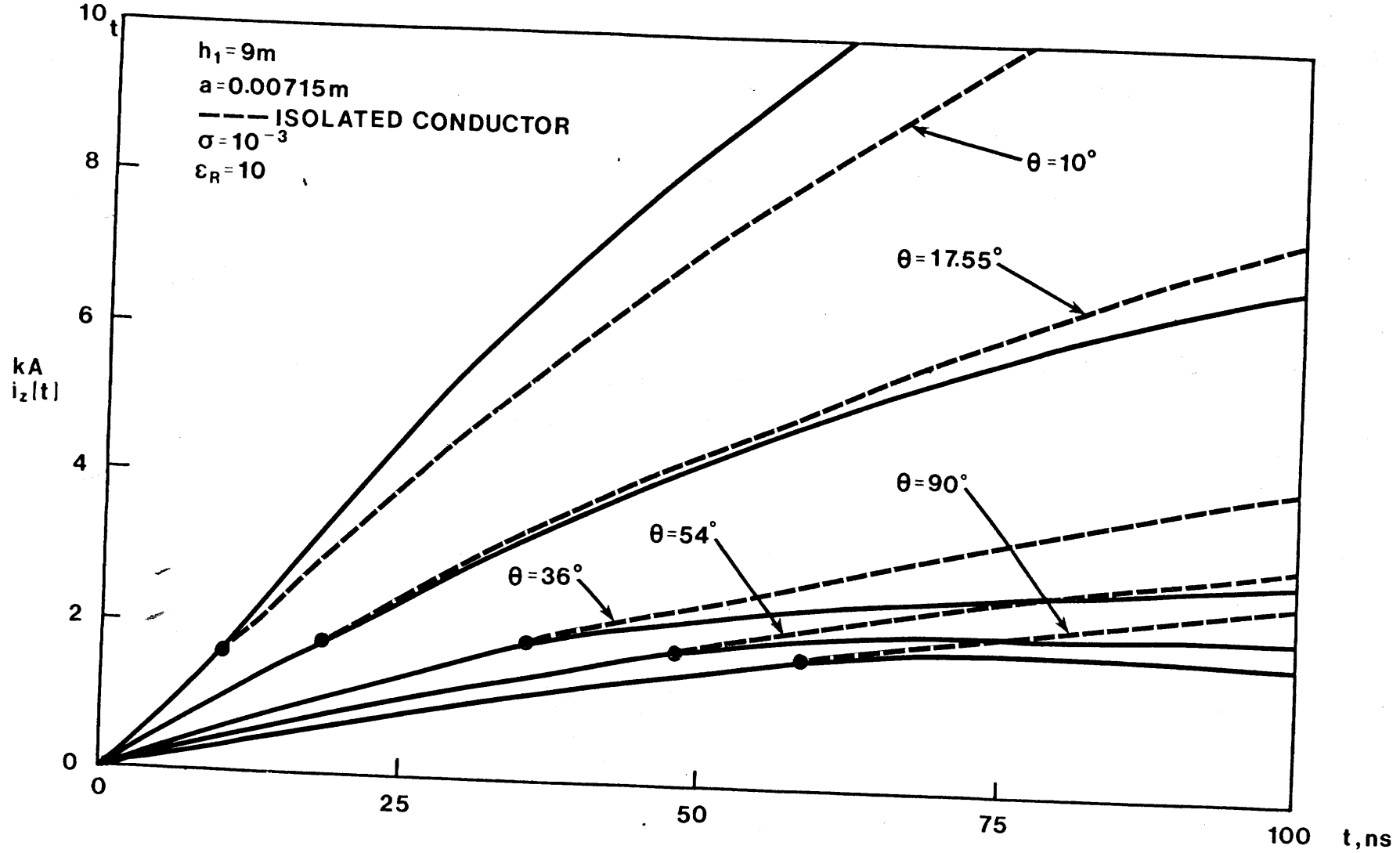

Figure 15. Time-domain current for a single wire above ground: $h_1 = 9m$, $a = 0.00715m$, $\sigma = 10^{-3}$, $\varepsilon_R = 10$.

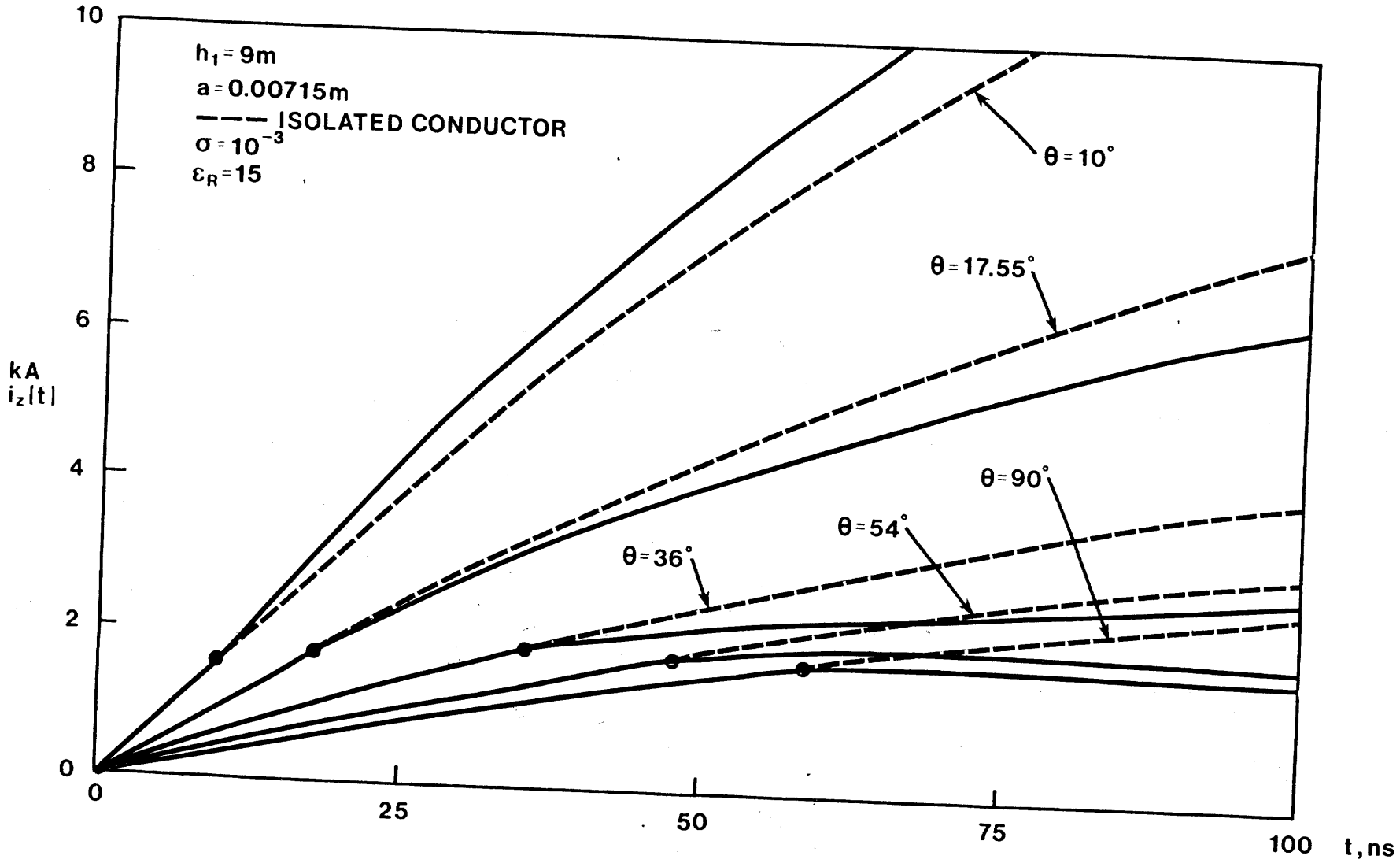

Figure 16. Time-domain current for a single wire above ground: $h_1 = 9m$, $a = 0.00715m$, $\sigma = 10^{-3}$, $\varepsilon_R = 15$.

are similar to those when only one wire is present, except that the overall currents are smaller here since the wire-to-wire coupling reduces the overall current as stated earlier.

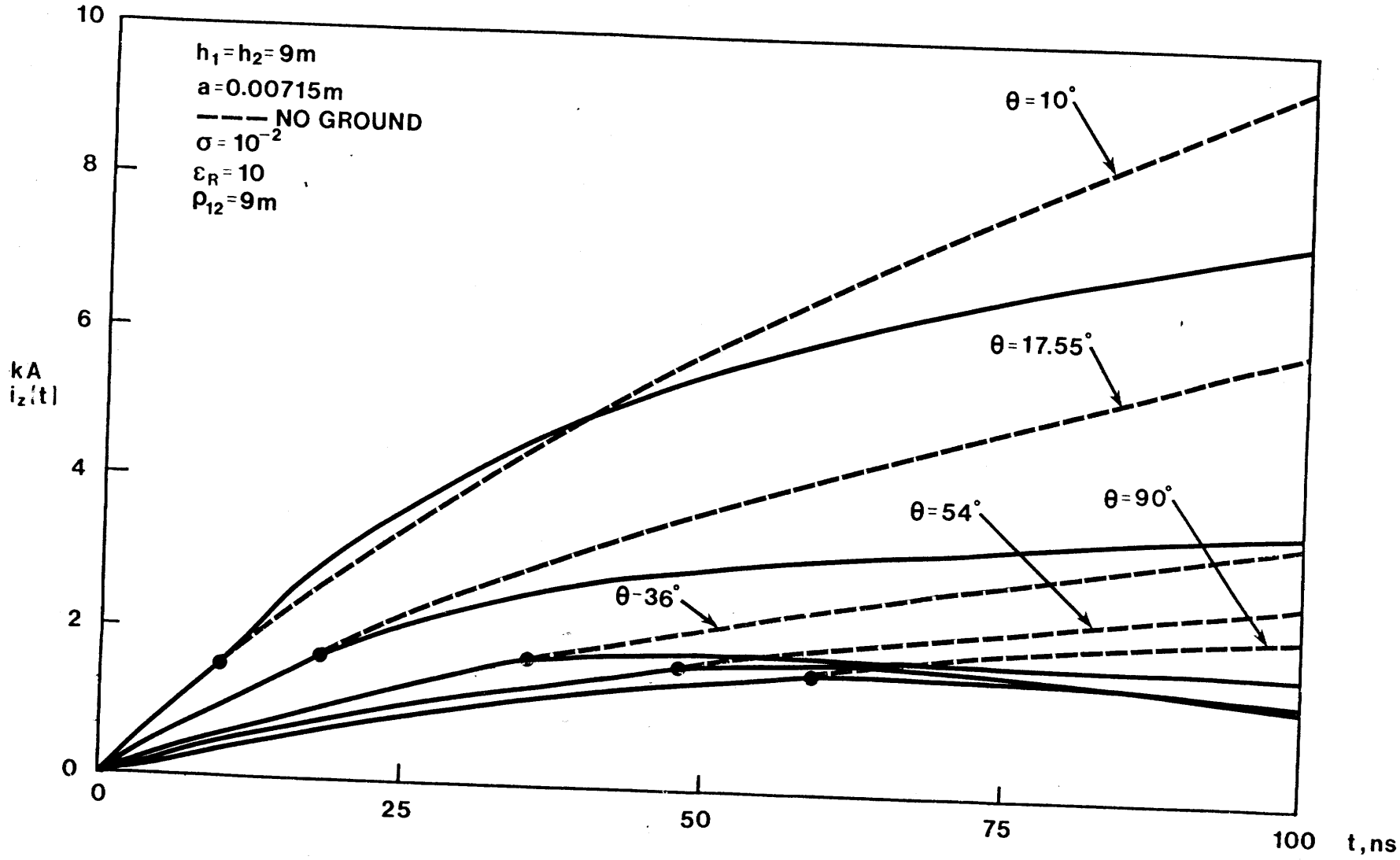

Figure 17. Time-domain current for two wires above ground: $h_1 = h_2 = 9m$ $a = 0.00715\,m$, $\rho_{12} = 9m$, $\sigma = 10^{-2}$, $\varepsilon_R = 10$.

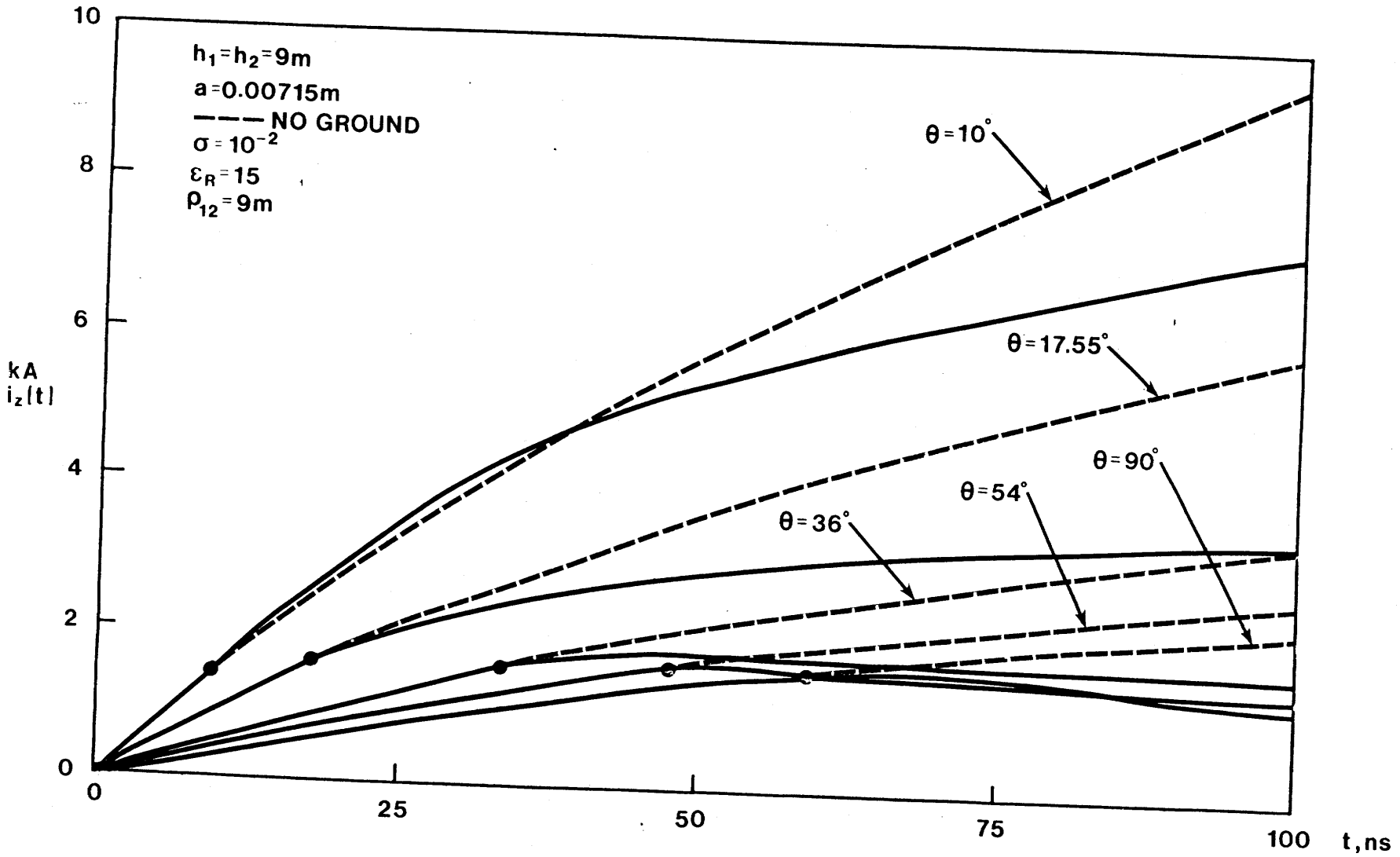

Figure 18. Time-domain current for two wires above ground: $h_1 = h_2 = 9m$, $a = 0.00715m$, $\rho_{12} = 9m$, $\sigma = 10^{-2}$, $\varepsilon_R = 15$.

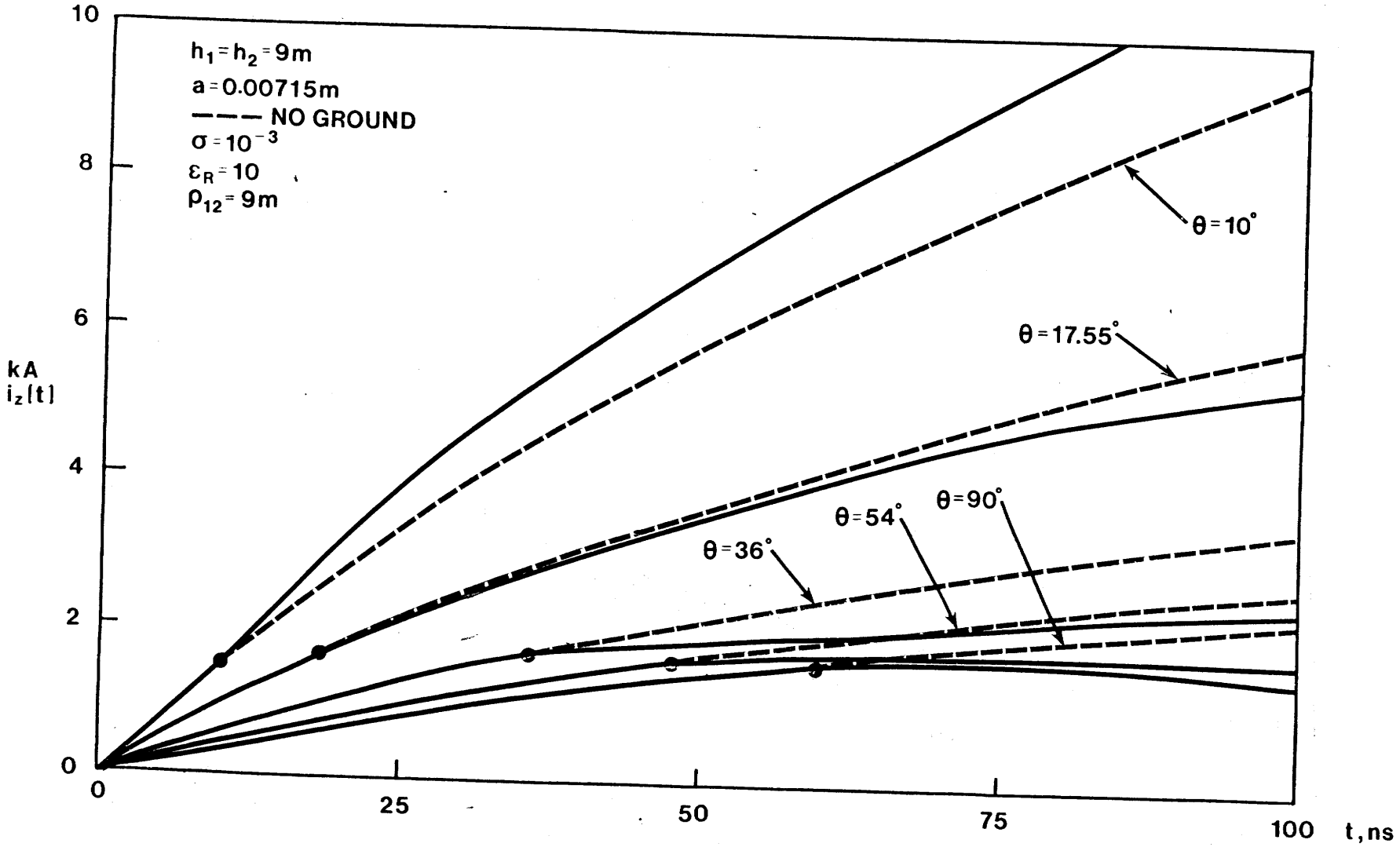

Figure 19. Time-domain current for two wires above ground: $h_1 = h_2 = 9m$, $a = 0.00715m$, $\rho_{12} = 9m$, $\sigma = 10^{-3}$, $\varepsilon_R = 10$.

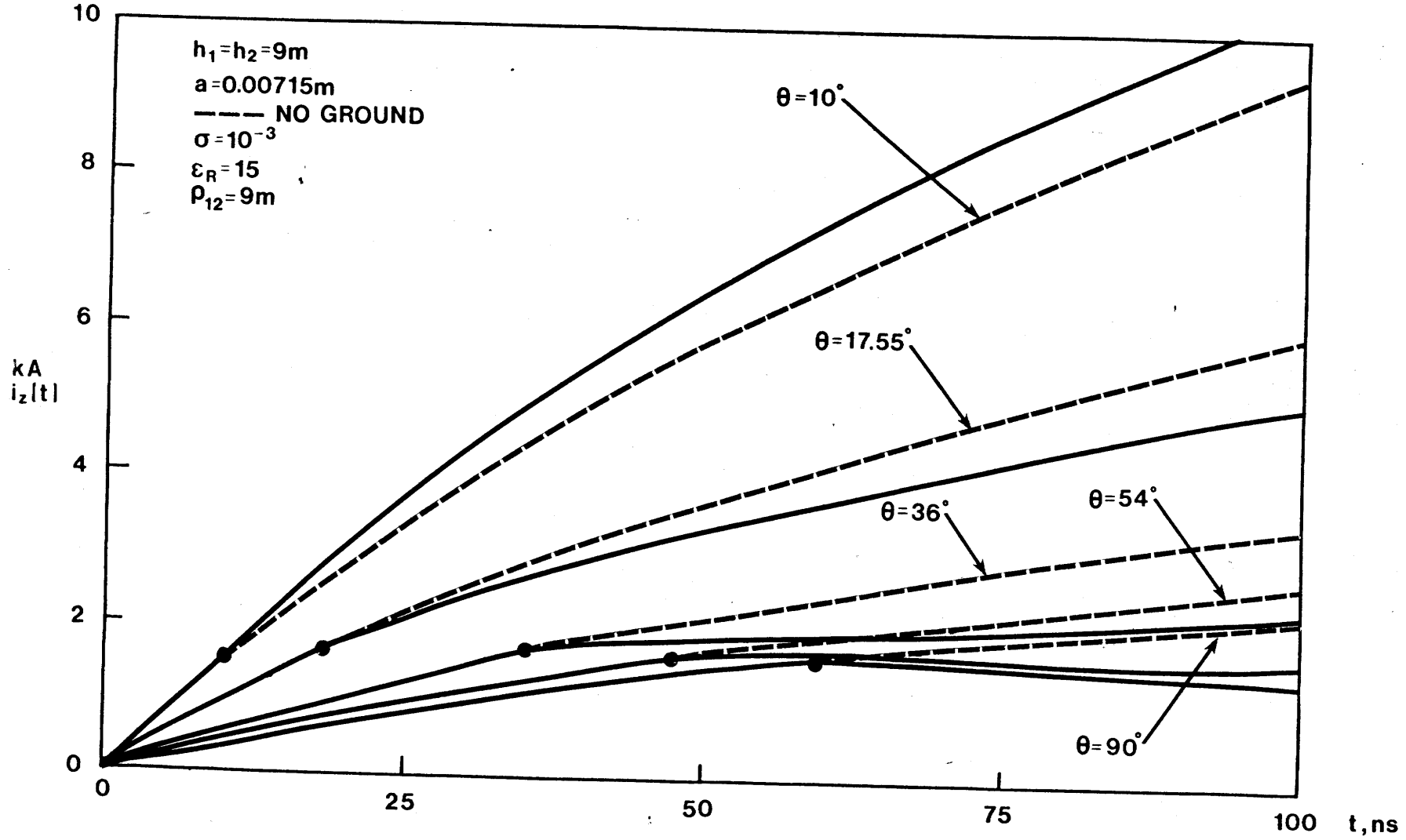

Figure 20. Time-domain current for two wires above ground: $h_1 = h_2 = 9m$, $a = 0.00715m$, $\rho_{12} = 9m$, $\sigma = 10^{-3}$, $\varepsilon_R = 15$.

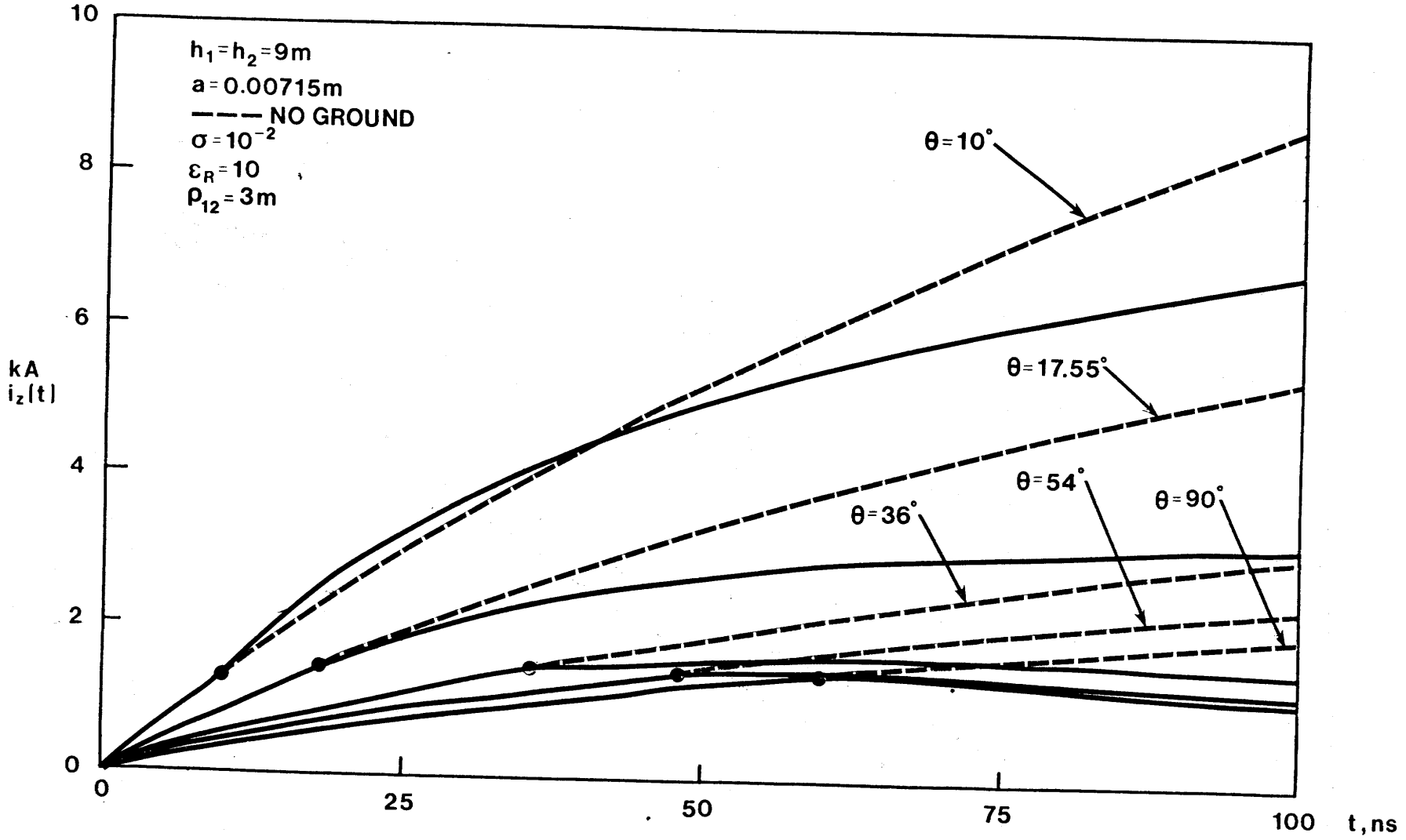

Figure 21. Time-domain current for two wires above ground: $h_1 = h_2 = 9m$, $a = 0.00715m$, $\rho_{12} = 3m$, $\sigma = 10^{-2}$, $\varepsilon_R = 10$.

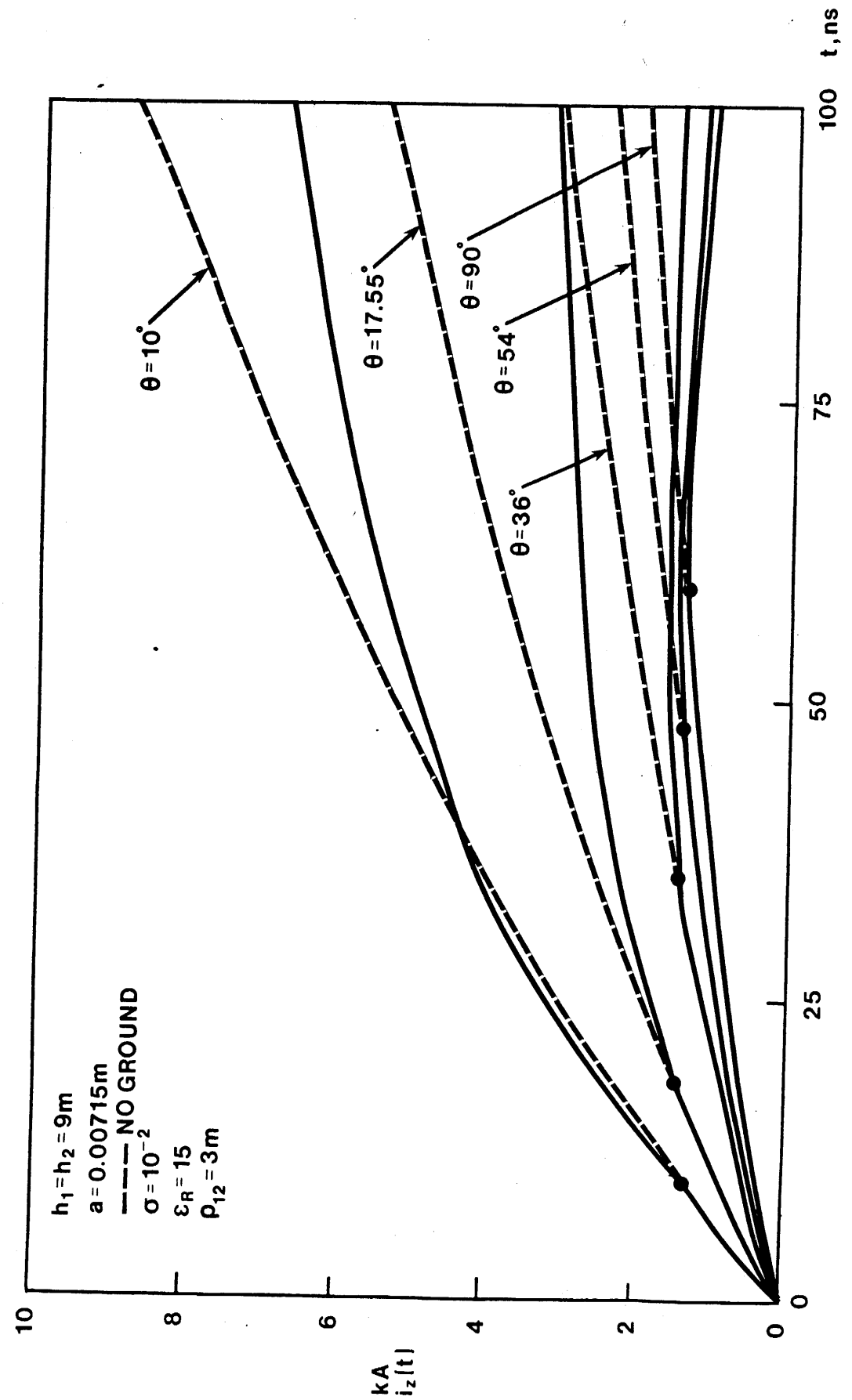

Figure 22. Time-domain current for two wires above ground: $h_1 = h_2 = 9m$, $a = 0.00715m$, $\rho_{12} = 3m$, $\sigma = 10^{-2}$, $\varepsilon_R = 15$.

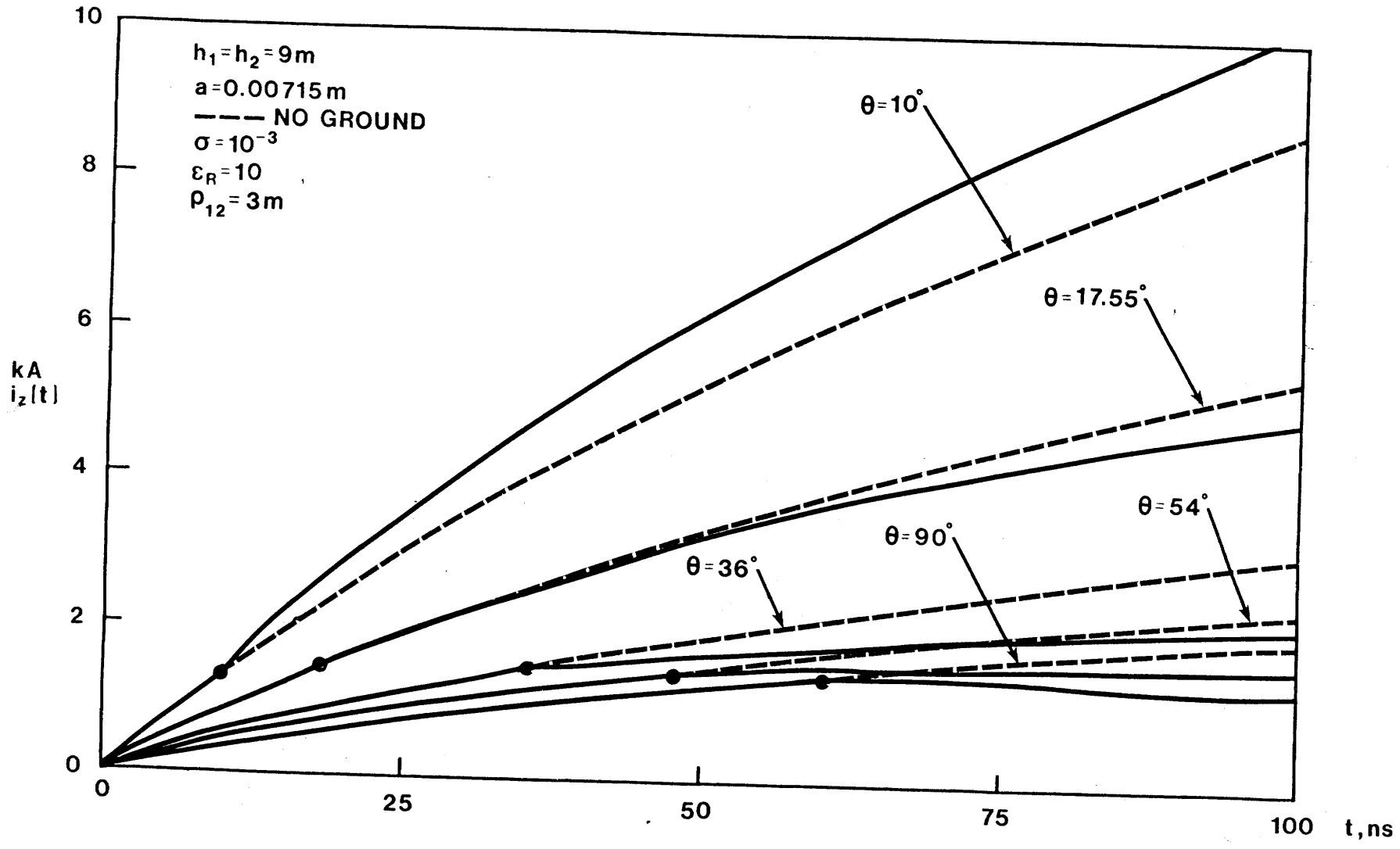

Figure 23. Time-domain current for two wires above ground: $h_1 = h_2 = 9m$, $a = 0.00715m$, $\rho_{12} = 3m$, $\sigma = 10^{-3}$, $\varepsilon_R = 10$.

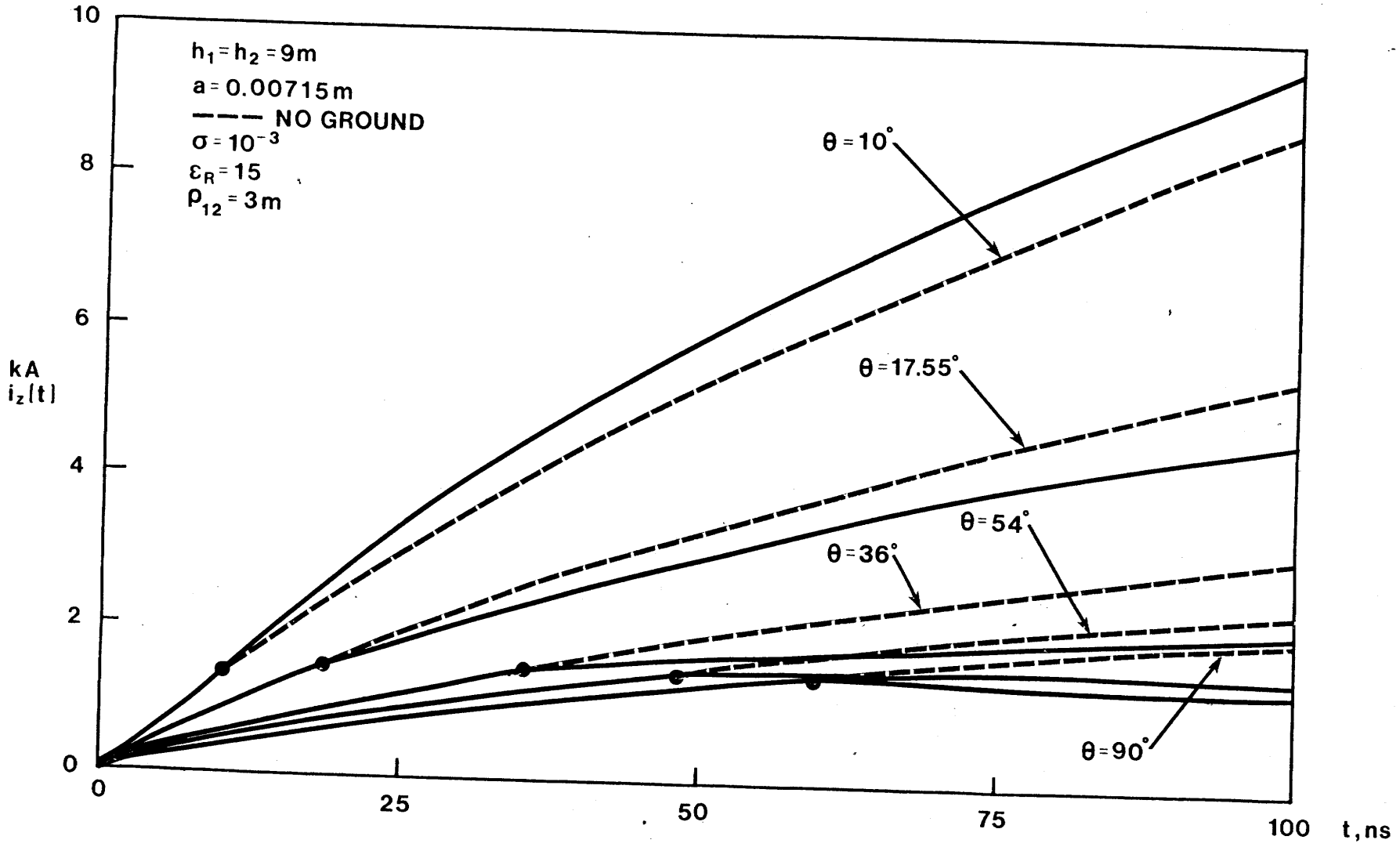

Figure 24. Time-domain current for two wires above ground: $h_1 = h_2 = 9m$, $a = 0.00715m$, $\rho_{12} = 3m$, $\sigma = 10^{-3}$, $\varepsilon_R = 15$.

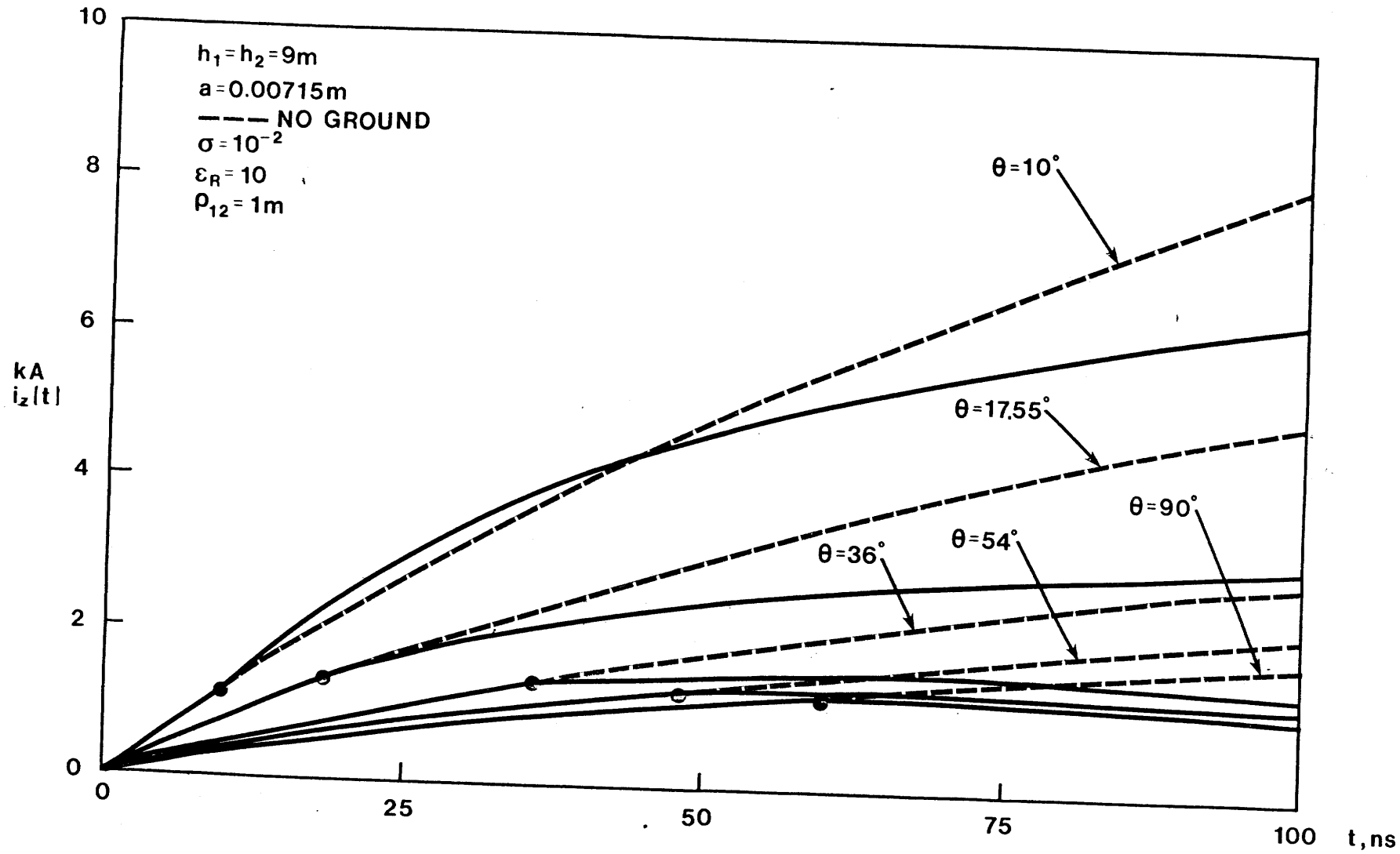

Figure 25. Time-domain current for two wires above ground: $h_1 = h_2 = 9m$, $a = 0.00715m$, $\rho_{12} = 1m$, $\sigma = 10^{-2}$, $\varepsilon_R = 10$.

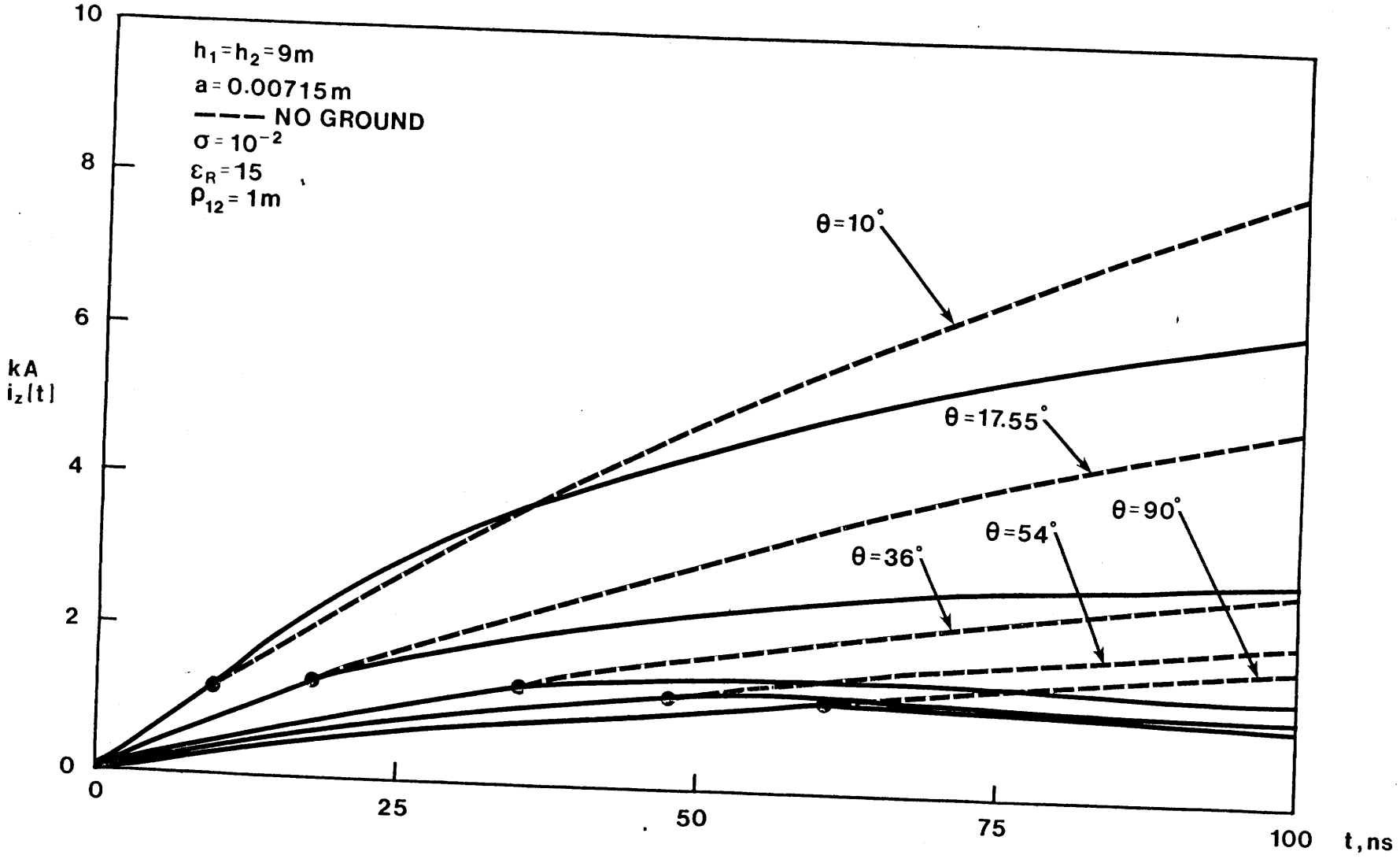

Figure 26. Time-domain current for two wires above ground: $h_1 = h_2 = 9m$, $a = 0.00715m$, $\rho_{12} = 1m$, $\sigma = 10^{-2}$, $\varepsilon_R = 15$.

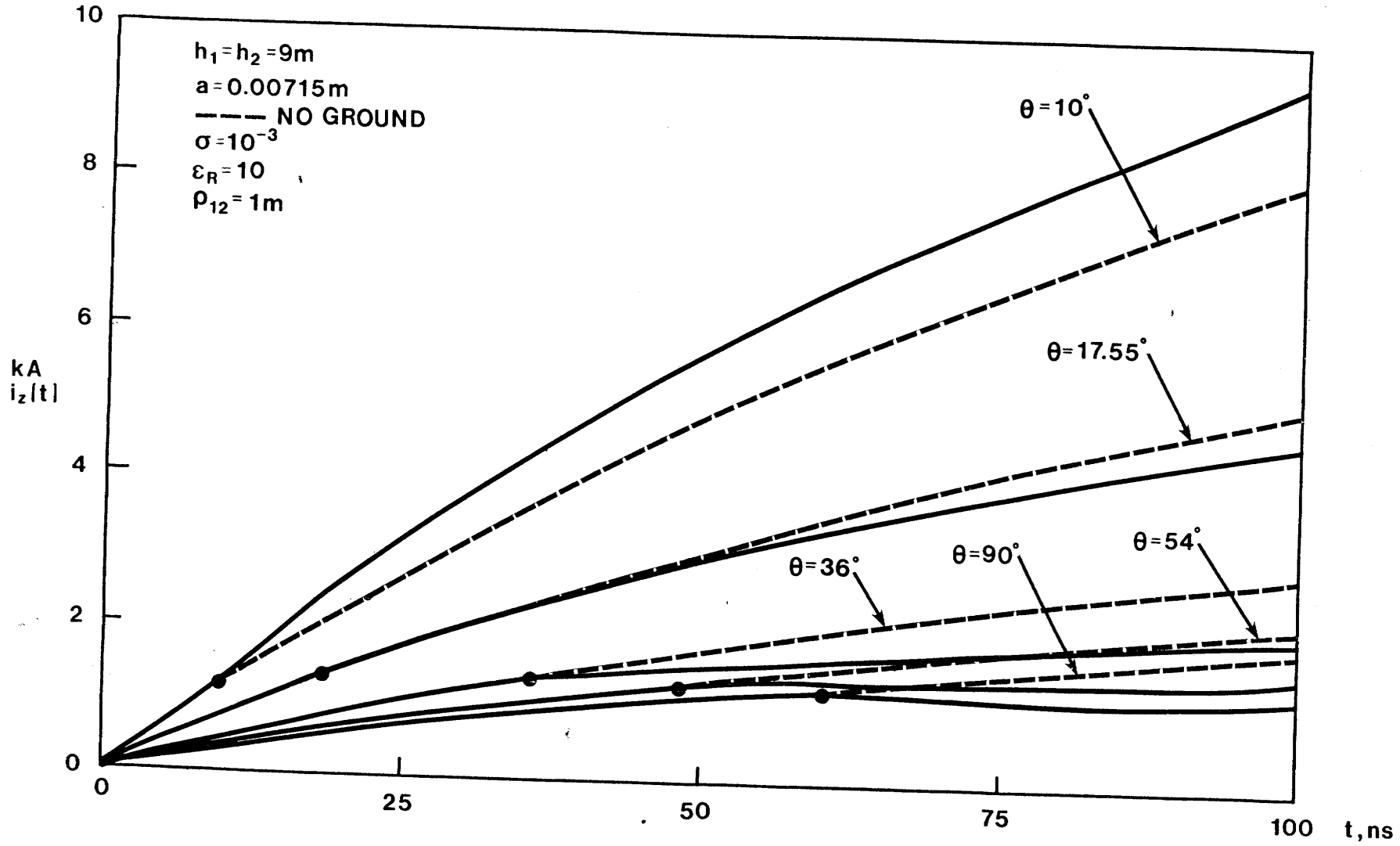

Figure 27. Time-domain current for two wires above ground: $h_1 = h_2 = 9m$, $a = 0.00715m$, $\rho_{12} = 1m$, $\sigma = 10^{-3}$, $\varepsilon_R = 10$.

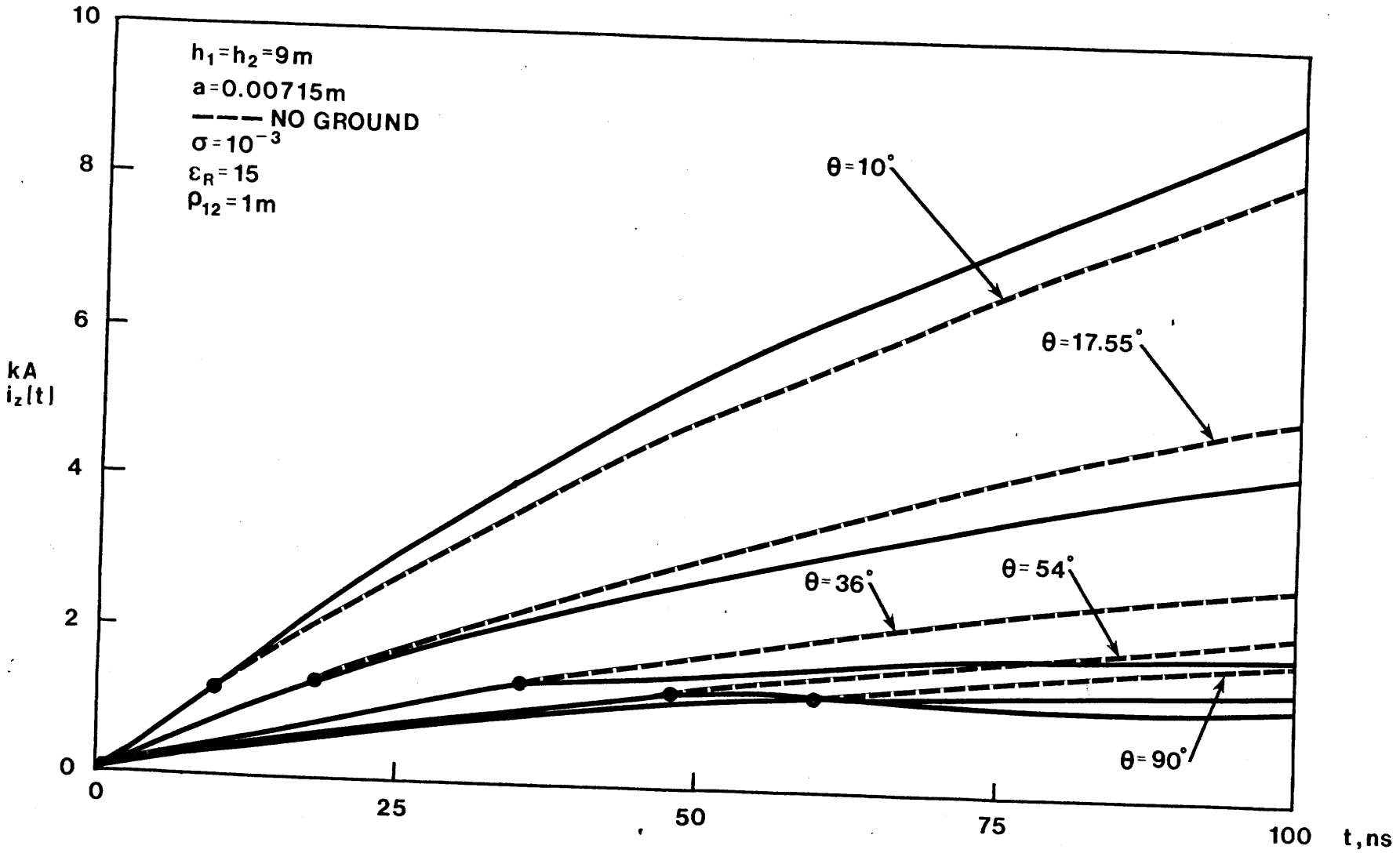

Figure 28. Time-domain current for two wires above ground: $h_1 = h_2 = 9m$, $a = 0.00715m$, $\rho_{12} = 1m$, $\sigma = 10^{-3}$, $\varepsilon_R = 15$.

VI. CONCLUDING REMARKS

Numerical time-domain results have been obtained for the current induced by an emp in one and two wires over both a perfectly conducting and finitely conducting plane earth for several cases of angle, conductivity, and permittivity. These results were obtained by taking the "boundary value problem" approach, and then making suitable and realistic approximations as the need arose. Results can easily be extended to the case of several parallel wires.

It has been found that for angles (θ) greater than the Brewster angle (θ_B) the currents reach peak values of about 2 kA in less than 100 ns for typical cases. For angles less than the Brewster angle the currents may reach peak values that are as large as 10 kA at times greater than 100 ns. This occurs because the current induced directly by the plane wave (emp) is large in itself, and, in addition, the ground reflected field adds to it ($\theta < \theta_B$).

The results presented in this work agree well with those of Lee[8] that were obtained using linear time-domain scattering theory in a somewhat simpler approach. The approximations that were made are essentially the same in both cases.

REFERENCES

[1] C. Flammer and H. E. Singhaus, "The Interaction of Electromagnetic Pulses With an Infinitely Long Conducting Cylinder Above a Perfectly Conducting Ground Plane," IN 144, 145, AFWL, August 1973.

[2] Handbook of Mathematical Functions, NBS, Series 55, June, 10964.

[3] P. R. Barnes, "The Axial Current Induced On an Infinitely Long, Perfectly Conducting, Circular Cylinder In Free Space by a Transient Electromagnetic Wave," IN 64, March 1971.

[4] K. S. H. Lee, editor, "EMP Interaction: Principles, Techniques and Reference Data," AFWL, December, 1980.

[5] H. P. Neff, Jr. and D. A. Reed, "Finitely Conducting, Infinitely Long, Cylindrical Wire in the Presence of a Plane Wave (EMP)," IN 436, February, 1984.

[6] H. P. Neff, Jr. and D. A. Reed," Plane Wave (EMP) Incidence on a Finitely Conducting Plane Earth with the Magnetic Field Intensity Parallel to the Earth's Surface," TN 351, February, 1984.

[7] R. G. Olsen and D. C. Chang, "Current Induced by a Plane Wave on a Thin Infinite Wire Near the Earth," IEEE Transactions on Antennas and Propagation, July, 1974.

[8] K. S. H. Lee, F. C. Yang and N. Engheta, "Interaction of High Altitude Electromagnetic Pulse (HEMP) with Transmission and Distribution Lines: an Early-Time Consideration," IN 435, December, 1983.

408 (49)

OAK RIDGE NATIONAL LABORATORY
OPERATED BY MARTIN MARIETTA ENERGY SYSTEMS, INC.

POST OFFICE BOX X
OAK RIDGE, TENNESSEE 37831

July 16, 1985

C. E. Baum
NTYEE
Kirkland AFB, NM 87117

Dear Carl:

All papers and notes submitted to AFWL for publication in the AFWL EMP Note Series are cleared for public release. We have clearance documentation on IN 441, IN 436, and TN 351. The documentation for IN 435 has been misfiled and we are attending to that problem.

Once again, all notes and papers that we submit to your office are cleared. A few notes by LuTech, Inc. will not be submitted to AFWL because of classification. If you have any further questions, please let me know.

Sincerely,

Kindy Barnes

P. R. Barnes

PRB/mm